HETEROCYCLES, Vol. 104, No. 8, 2022, pp. 1373 - 1413. © 2022 The Japan Institute of Heterocyclic Chemistry
Received, 9th April, 2022, Accepted, 23rd May, 2022, Published online, 30th May, 2022
DOI: 10.3987/REV-22-982

NON-PLANAR POLYCYCLIC AROMATIC MOLECULES INCLUDING HETEROLE UNITS

Koki Kise[1] and Takayuki Tanaka[2]*

[1] Department of Chemistry, Graduate School of Science, Kyoto University, Kitashirakawa Oiwake-cho, Sakyo-ku, Kyoto 606-8502, Japan. [2] Department of Molecular Engineering, Graduate School of Engineering, Kyoto University, Kyotodaigaku Katsura, Nishikyo-ku, Kyoto 615-8195, Japan; e-mail:tanaka@moleng.kyoto-u.ac.jp

Abstract – Recent developments in non-planar polycyclic aromatic molecules bearing heterole units have been reviewed, including internally and externally heteroatom doped corannulenes, rim and benzylic heteroatom doped sumanenes, hexapyrrolohexaazacoronenes, and hetero[n]circulenes.

CONTENTS

1. INTRODUCTION

An ideal Hückel aromatic compound is defined to possess [4n+2]π electron cyclic conjugation in a planar platform as the most typically represented by benzene. This is essentially applicable to polycyclic aromatic compounds. Most of polycyclic aromatic hydrocarbons (PAHs) such as acenes, pyrenoids and coronoids, as well as porphyrins and phthalocyanines, possess planar structures to attain effective conjugation and thereby aromatic stabilization. Recent developments in synthetic organic chemistry enabled to enforce them into non-planar ones mainly by embedding non-hexagonal rings, steric strain from atom crowding, and ring contraction/expansion. As a result, molecules have been transformed to bowl, saddle, sphere, hoop, helix, and even Möbius shaped structures (Figure 1).[1-5] These curved polycyclic molecules have been a recent appealing research topic in terms of templates for 3D nanocarbons,[2] aromaticity associated with topology,[3] chiroptical properties,[4] and materials applications.[5] In particular, bowl shaped PAHs such as corannulene and sumanene have been attracting significant attention due to their structural relevance to fullerenes and cap structures of carbon nanotubes.[6] Historically, corannulene was first synthesized by Barth and Lowton in 1966[7] and sumanene was first synthesized by Sakurai and Hirao in 2003.[8] Several reviews focusing on the synthesis of these bowl shaped molecules were published elsewhere.[6]

In the last decade, further chemical modifications on these planar and non-planar PAHs have been achieved by specific heteroatom doping.[9] The heteroatom doped PAHs can acquire peculiar properties otherwise unattainable, such as redox property, intramolecular charge-transfer character, and Lewis acidity (Figure 2).[10] In this review, we will introduce emerging heteroatom doped non-planar polycyclic aromatic molecules, especially focusing on heteroatom doped corannulenes and sumanenes. In addition, a novel class of heterole embedded polycyclic aromatic molecules such as hexapyrrolohexaazacoronene and hetero[n]circulenes are highlighted. To limit the scope, heterocycles other than five-membered ring (for example, pyridine and azepine) are not fully included.

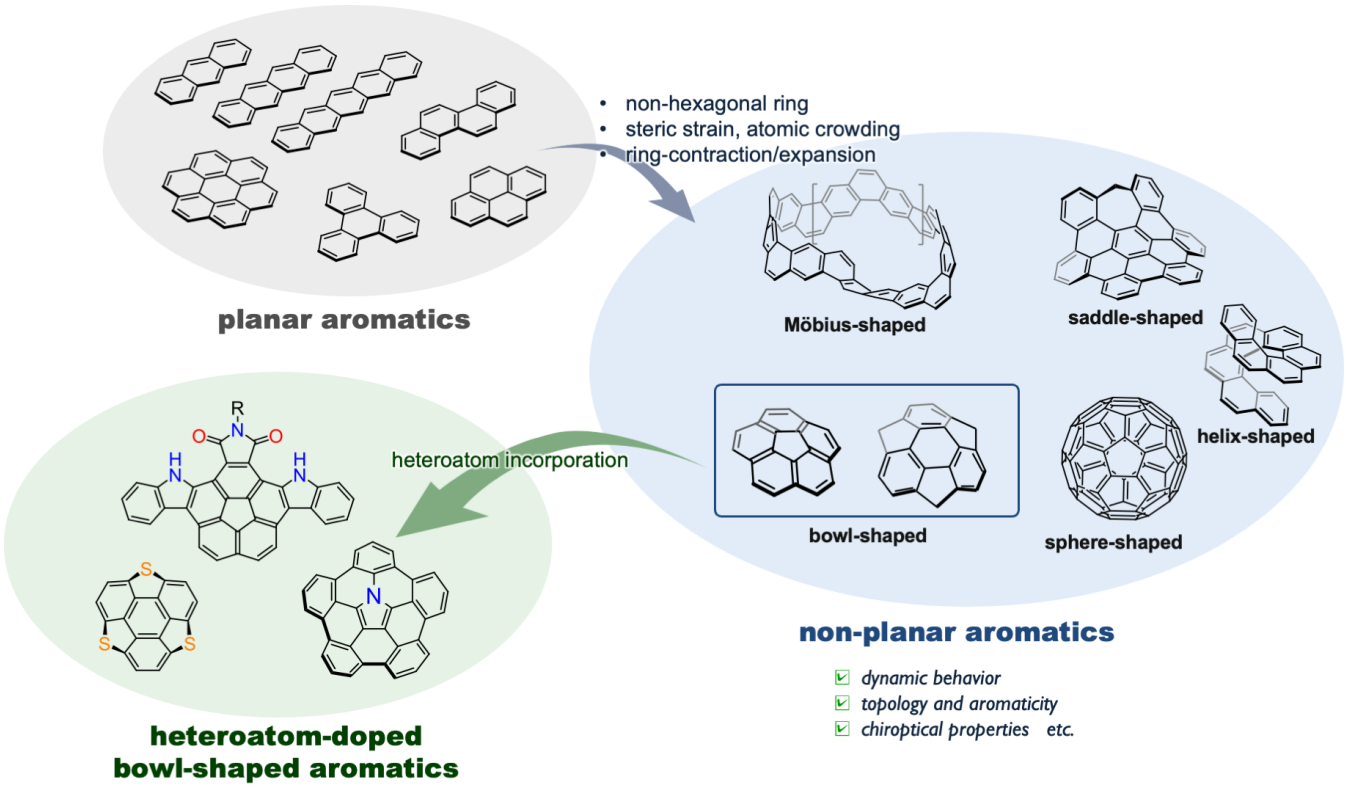

Figure 1. Planar and non-planar aromatics and their heteroatom incorporation

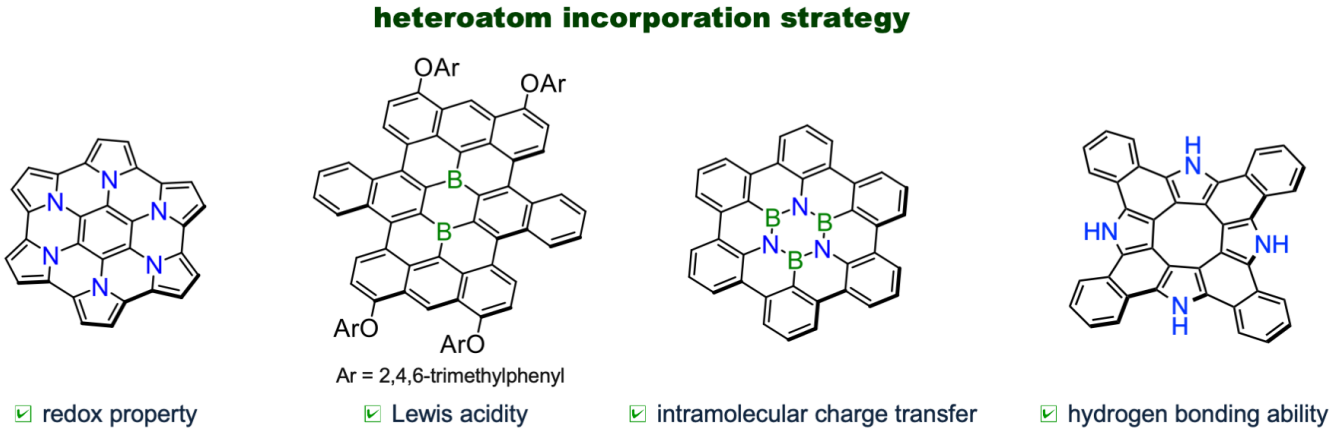

Figure 2. Heteroatom incorporation strategy and peculiar properties derived from the doped heteroatoms

2. CORANNULENE

Corannulene ($C_{20}H_{10}$) is a C_{5v} symmetric bowl shaped PAH in which a five-membered ring at the center is surrounded by five fused benzene rings.[7] It is regarded as the peripherally hydrogenated substructure of Buckminsterfullerene C_{60}, but its curvature is more relieved than that of C_{60} as indicated by their π-orbital axis vector (POAV) angles; 8.2° for corannulene and 11.6° for C_{60}.[11] Four different types of bonds in corannulene are referred to as spoke, hub, flank, and rim as shown in Figure 3. The bond lengths of spoke

and rim (~1.38 Å) are shorter than those of hub and flank (1.41–1.44 Å). The bowl depth of corannulene, which is the distance between the centroid of the central five-membered ring and the mean-plane defined by the peripheral ten rim carbon atoms, is 0.87 Å. Resulting from its bowl shaped structure, corannulene owns convex and concave π-surfaces and its dipole moment is 2.1 Debye, the direction of which is perpendicular to the central pentagon. Another characteristic feature derived from the bowl shaped geometry is bowl-to-bowl inversion dynamics. Two bowl shaped equilibrium structures are connected via a planar transition state. The inversion barrier of the pristine corannulene is *ca*. 10 kcal mol^{-1}. The energy barrier is dependent on the peripheral substituents, and the bowl is flattened by bulky substituents or fused rings in some cases.[12]

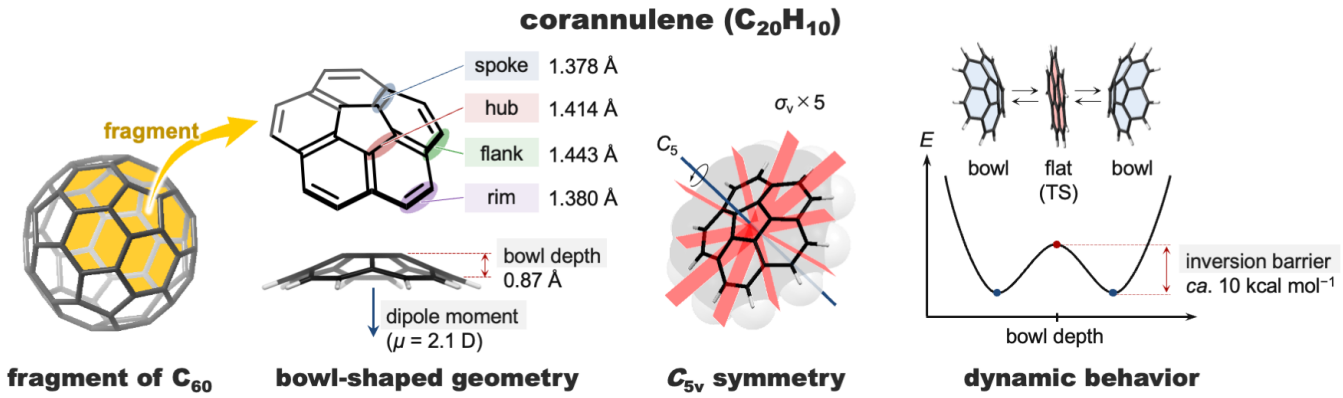

Figure 3. Structural relevance to C_{60}, the bowl shaped geometry, C_{5v} symmetry, and dynamic behavior of corannulene

The first synthesis of pristine corannulene by Barth and Lowton provided less than 1% yield over 17 steps from 1,2-dihydroacenaphthylene (**1**) (Scheme 1).[7] For a long time, corannulene was not recognized as an important research target before the preparation and extensive characterization of fullerene was achieved in 1990s. In 1991, Scott *et al*. developed a synthetic protocol of corannulene using flash vacuum pyrolysis (FVP).[13,14] The advantage of this route is short synthetic steps and improved yield: 20–25% total yield over 3 steps from acenaphthylene-1,2-dione (**2**). As a result, gram-scale synthesis of corannulene became possible and the importance of corannulene was recognized not only as a fragment of C_{60}, but also as a non-planar PAH. However, there were still a few disadvantages of the FVP method: 1) no functional group tolerance, 2) unexpected thermal rearrangements, and 3) undesired side reactions at high temperature (1100 °C). Later, Siegel's group has reported a kilogram-scale synthesis of corannulene by all in-solution reactions in 2012. They optimized reaction conditions to reduce costly and toxic reagents, and avoided purification by column chromatography as much as possible.[15] Then, an acceptable yield of 8.7% over 9 steps from 1-(chloromethyl)-3-methylbenzene (**3**) has been achieved. Recently, further efforts have been

made on the preparation of corannulene and the mechanochemical conditions using ball mills have been reported.[16]

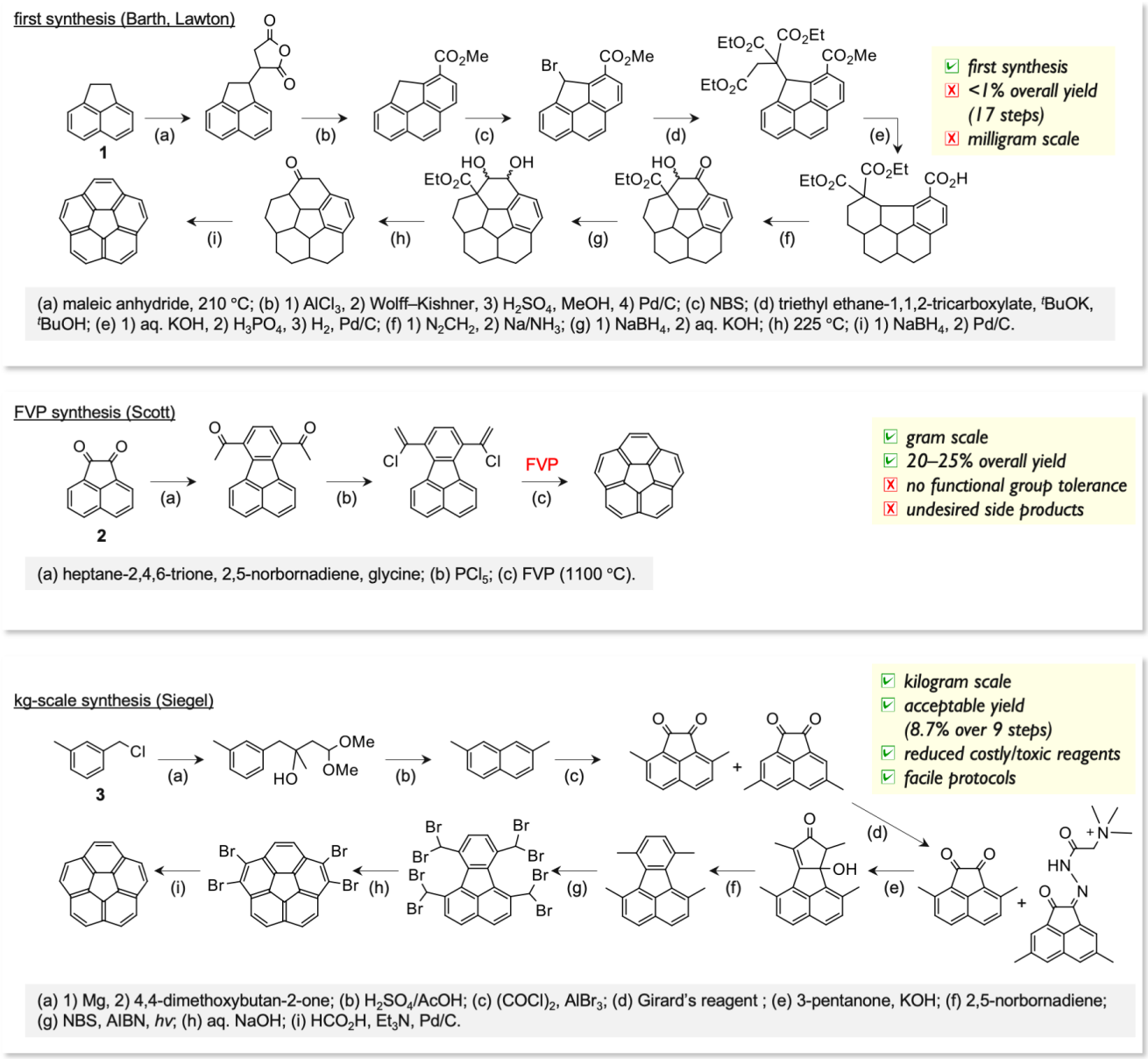

Scheme 1. Development of synthetic protocols to prepare the pristine corannulene

Recently, heteroatom incorporation to corannulene has been achieved to perturb its electronic properties and to construct model compounds for heterafullerenes.[17] Reported heteroatom doped corannulenes can be categorized into 1) internally heteroatom doped corannulenes and 2) externally heteroatom doped ones (Figure 4). Here, the internal incorporation means that carbon atom(s) in the corannulene framework is/are substituted with heteroatom(s) and the external incorporation means that the corannulene scaffold is π-

extended with heteroatom containing aromatic unit(s). To date, internally doped atoms are only nitrogen and boron, while externally fused heterole units are furan, pyrrole, and thiophene.

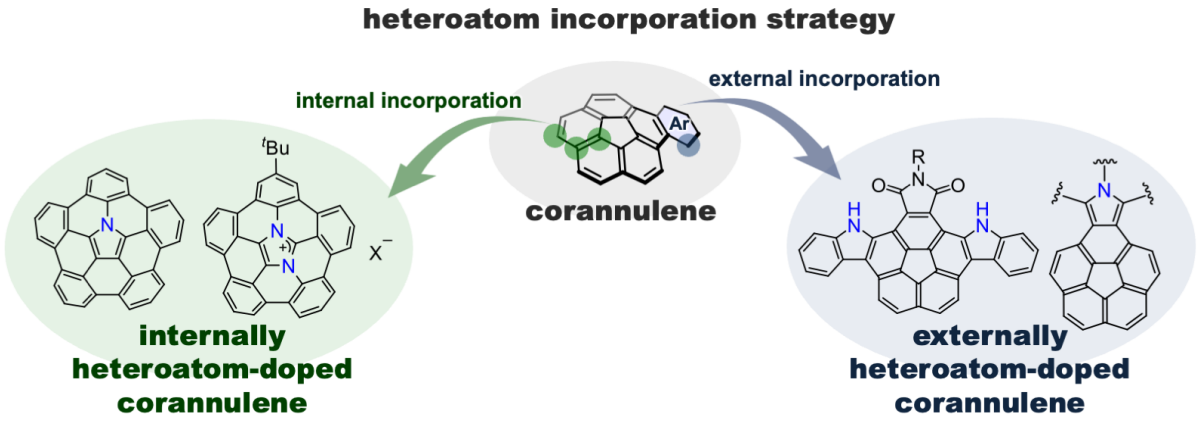

Figure 4. Two categories of nitrogen doped corannulene: internal or external incorporation

2-1. INTERNALLY HETEROATOM DOPED CORANNULENE

After several unsuccessful attempts,[18] Scott *et al*. have succeeded in the synthesis of azadibenzocorannulene **5** from a nitrogen-containing precursor **4** by a FVP approach in 28% yield (Scheme 2a).[19] Owing to the shorter lengths of C–N bonds, the hub carbon atoms of **5** possess an average POAV angle of 8.30°, which is approximately 1° larger than that of its carbon analogue **8** (7.33°). Thus, azabowl **5** was prone to suffer ring opening by hydrolysis on silica-gel or by the thermal bond cleavage to afford **6** and **7**, respectively. This is the first example of azacorannulene in which a carbon atom on the rim is substituted with a nitrogen atom.

In 2018, Hatakeyama *et al*. reported the synthesis of B_2N_2 embedded corannulene **13** (Scheme 2b).[20] Commercially available 4,7-dibromobenzo[*c*][1,2,5]thiadiazole (**9**) was capped with phenylboronic acid, and the sulfur extrusion reaction of resultant thiadiazole **10** followed by condensation with 2,2-diphenylacetic acid under heating afforded **12**. Finally, electrophilic C–H borylation of **12** with BBr_3 in *o*-dichlorobenzene at reflux gave the desired product **13**. The total yield was 25% in four steps and multigram preparation (~3.6 g) was possible. This BN doped corannulene **13** was fairly stable in the air and did not decompose even at 350 °C. Notably, **13** exhibits intense blue fluorescence with a large quantum yield (Φ_F = 0.69) compared with the pristine corannulene ($\Phi_F \leq 0.07$). As an application, the group fabricated the first corannulene based organic light emitting diode (OLED), affording an external quantum efficiency of 2.61%.

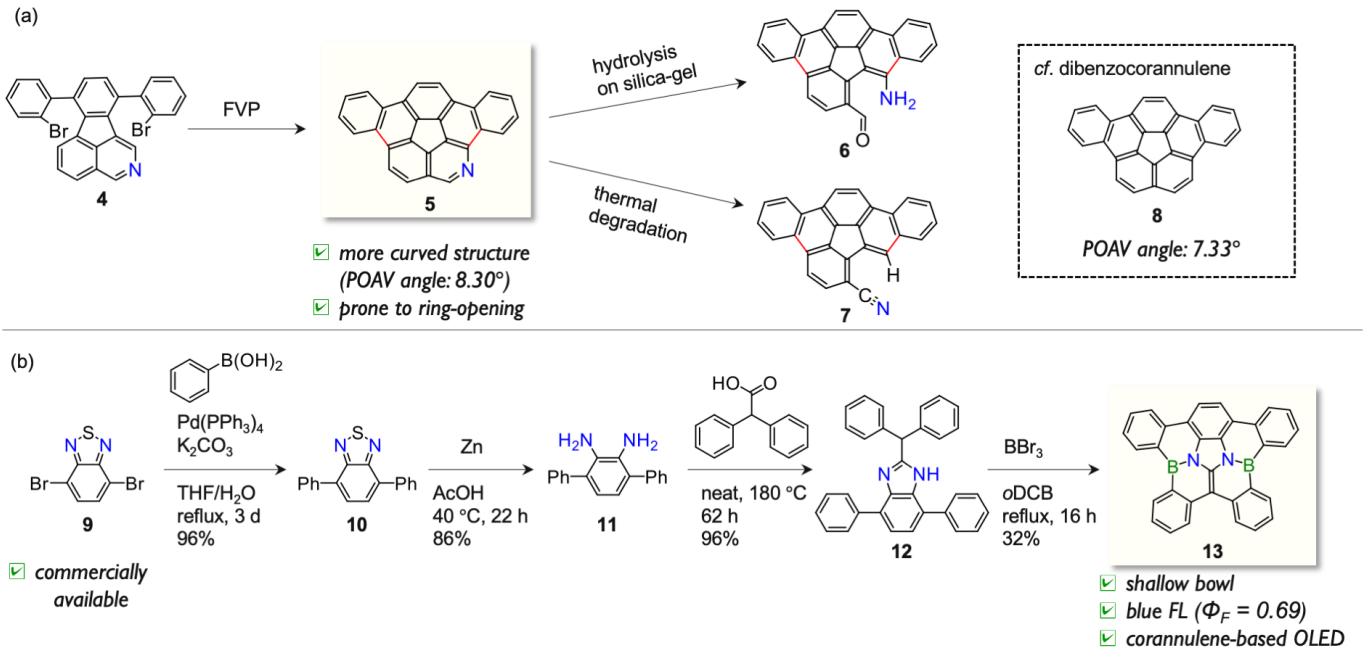

Scheme 2. Synthesis of internally heteroatom doped corannulenes (a) FVP approach toward azacorannulene (b) Short-step synthesis of B_2N_2 doped corannulene

In 2015, Hiroto, Shinokubo *et al.*[21] and Ito, Nozaki *et al.*[22] independently reported substituted derivatives of a pentabenzoazacorannulene, **21a** and **21b**, respectively, in which a pyrrolic nitrogen atom is located at the central five-membered hub position (Scheme 3a). They have established totally different routes toward **21a** and **21b**, except that the last step was palladium catalyzed intramolecular arylative cyclization reaction in both cases. For **21a**, tetrabenzocarbazole **15** was subjected to the intramolecular cyclization to make a C–C bond, giving rise to a distorted double-helicene-like molecule **16**. After selective tribromination, the same cyclization reaction gave pentabenzoazacorannulene **21a** in 46% yield. For **21b**, Ito, Nozaki *et al.* utilized polycyclic aromatic azomethine ylide, which was generated from iminium salt **18a**·HCl by the method independently developed by the same group[23] and Feng/Müllen's group.[24] The 1,3-dipolar cycloaddition reaction of the azomethine ylide **18a** with 2,2',6-trichlorodiphenylethyne (**19**) and subsequent oxidative dehydrogenation afforded a precursor **20**. Then, palladium catalyzed intramolecular cyclization of **20** gave **21b** in 14% yield. Owing to the doped nitrogen atom, the oxidation potential of **21a** ($E_{ox.}$ = 0.20 V *v.s.* Fc/Fc$^+$) is significantly lower than that of pristine corannulene ($E_{ox.}$ = 1.57 V *v.s.* Fc/Fc$^+$). This electron-rich nature brings two consequences (Figure 5): 1) facile generation of oxidized species and 2) favorable association with fullerenes. As for the former, **21a** can be oxidized under air in the presence of trifluoroacetic acid to form its radical cation **21a**$^{\bullet+}$. Interestingly, **21a**$^{\bullet+}$ underwent reversible σ-bond formation to afford dimeric azacorannulene **25**.[25] As for the latter, electron-rich azacorannulene **21a** has a larger association constant with C_{60} ($K_a = 6.2\times10^4$ M^{-1} in toluene) than pristine corannulene ($K_a < 1$ M^{-1} in

benzonitrile).[26] In addition, co-crystals of **21a** and C_{60} exhibited significantly high charge mobility of 0.17 $cm^2\ V^{-1}\ s^{-1}$ compared with only **21a**. Moreover, the group of Shinokubo designed dimeric azacorannulene **26** and **27a**,**b**, aiming at much stronger associative interactions with fullerenes.[26] The directly linked dimer **26** acts as a C_{60} host with concentration-dependent stoichiometry. In other words, **26** forms one-dimensional chain-like fibre aggregates with a 1:1 host-guest ratio in the presence of equimolar C_{60}, whereas it forms crystals with a 1:2 ratio in the presence of excessive C_{60}. The azabuckybowl based molecular tweezers **27a**,**b** act as effective receptors for C_{70} and C_{60}, respectively, with top class association constants ($K_a > 10^7$ M^{-1} in toluene) for bowl shaped molecules, enabling even purification of **27b·C$_{60}$** with silica-gel column chromatography. It is reminiscent of the fact that corannulene dimer **28**, known as a buckycatcher, shows more than 1000 times larger association constant with C_{60} ($K_a = 8.6\times10^3$ M^{-1} in toluene) than the pristine corannulene. The K_a values of **27a**,**b** are even larger than that of **28** due to their electron-donating characters ascribable to the doped nitrogen atoms. The 1:1 assembly of **27a**,**b** and fullerenes can be seen as a donor-acceptor-donor (D-A-D) system. Such a supramolecular D-A-D system is expected to exhibit the enhanced two-photon absorption (TPA) cross section since quadrupolar characteristics are generated due to the intramolecular charge transfer. As expected, **27a**,**b** exhibited enhanced TPA cross section value of over 200 GM upon binding of C_{60}.

Very recently, Xing, Ito *et al*. have reported diazapentabenzocorannulenium salts **24a**,**b** (Scheme 3b).[27] The synthesis of **24a** was achieved by the 1,3-dipolar cycloaddition reaction of 6-chlorophenathridine (**22**) and polycyclic azomethine ylide generated from **18b**·HCl, via a nitrilium salt intermediate, followed by palladium catalyzed intramolecular arylative cyclization reaction. Despite the lack of hydrophilic substituents, **24a** is well soluble in various solvents including water owing to its cationic charge, doped nitrogen atoms, and bowl shaped structure. In addition, **24a** is selectively localized in the mitochondria of tumor cells, enabling its application as a fluorescent cellular probe.

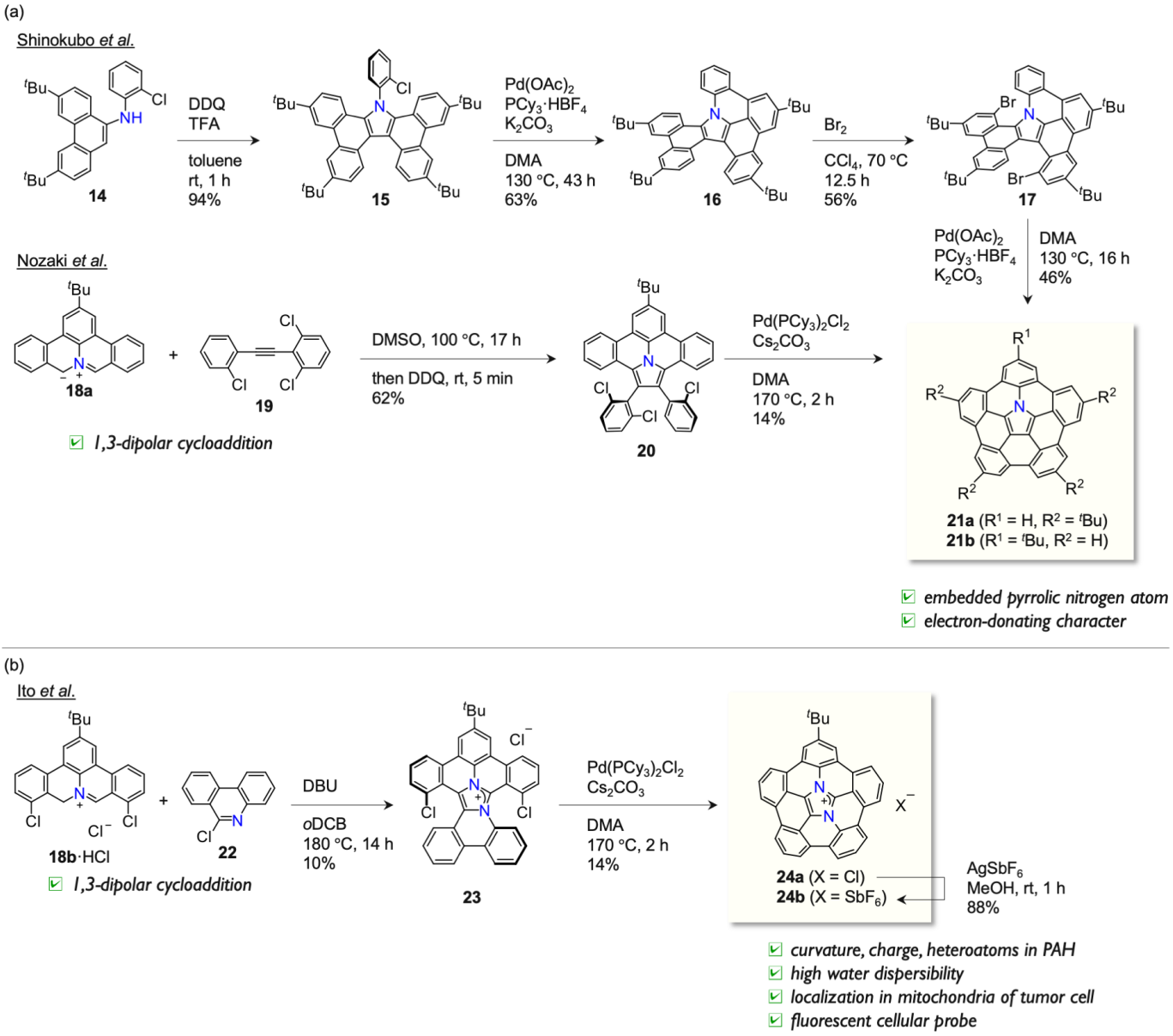

Scheme 3. Internally heteroatom doped corannulenes (a) Electron-rich azacorannulene and its related derivatives as host molecules for electron-deficient fullerenes (b) Hydrophilic and biophilic cationic buckybowl

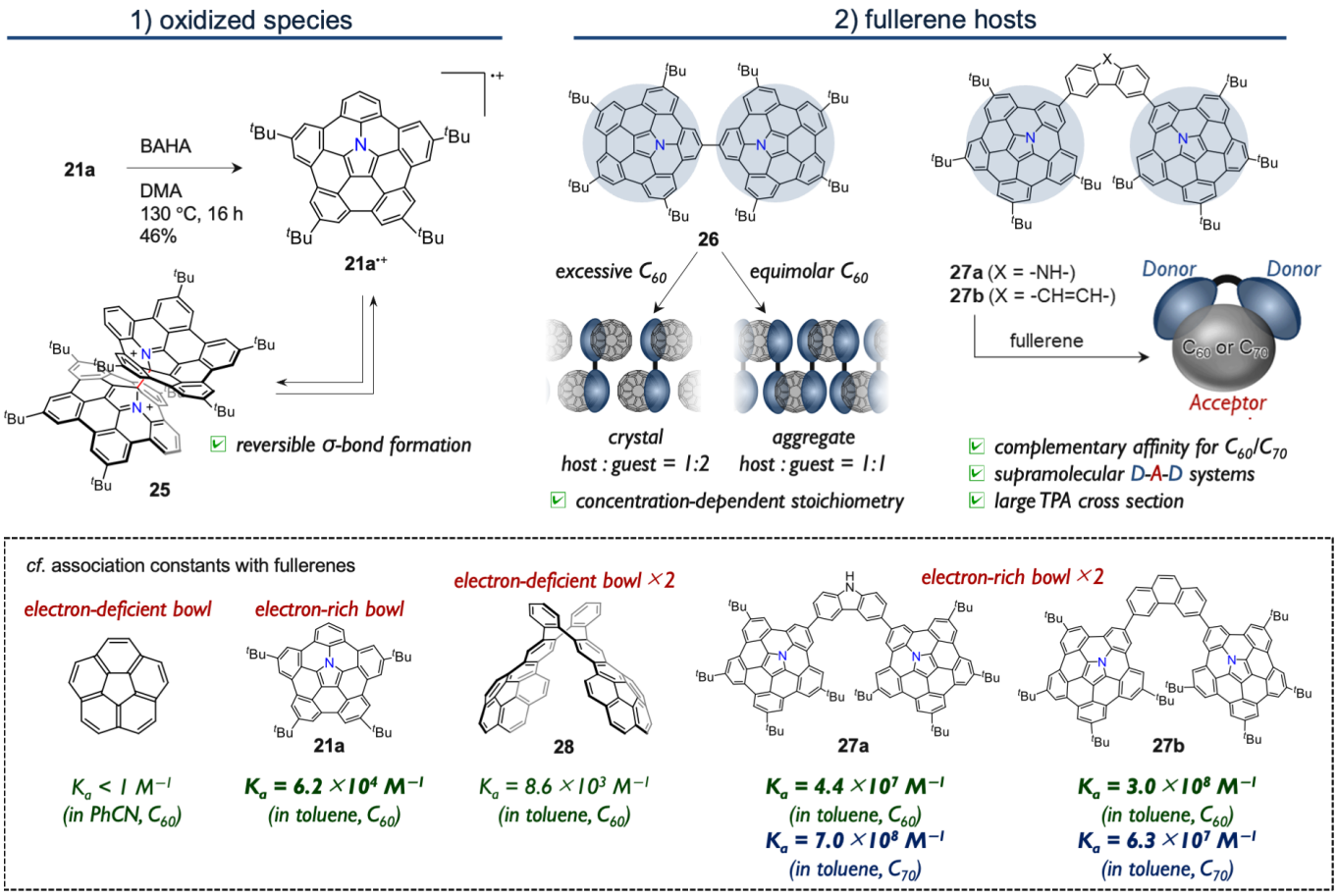

Figure 5. Reversible σ-bond formation and host-guest chemistry of dimeric azacorannulenes

2-2. EXTERNALLY HETEROATOM DOPED CORANNULENE

The peripheral functionalization of corannulene derivatives have been utilized to develop novel functional materials. For instance, they are applied to non-fullerene acceptor and supramolecular polymerization.[28] Ito and Nozaki *et al*. synthesized singly and doubly pyrrole fused corannulenes **29** and **30** by applying the two step reaction sequence involving 1,3-dipolar cycloaddition of the *in situ* generated polycyclic azomethine ylide **18a** with corannulene, and the subsequent oxidative aromatization (Scheme 4a).[29] This is the first example of a 1,3-dipolar cycloaddition in which the rim bond of corannulene serves as a dipolarophile. The fused corannulene **29** and **30** exhibit solvatofluorochromism due to the intramolecular charge transfer. The same group extended the protocol to construct corannulene–azacorannulene hybrid **32** by applying the above-mentioned cyclization reaction, followed by palladium catalyzed intramolecular C-H arylation.[30] Azabuckybowl **32** is highly curved and its maximum POAV angle (11.3°) is comparable to that of C_{60} (11.6°).

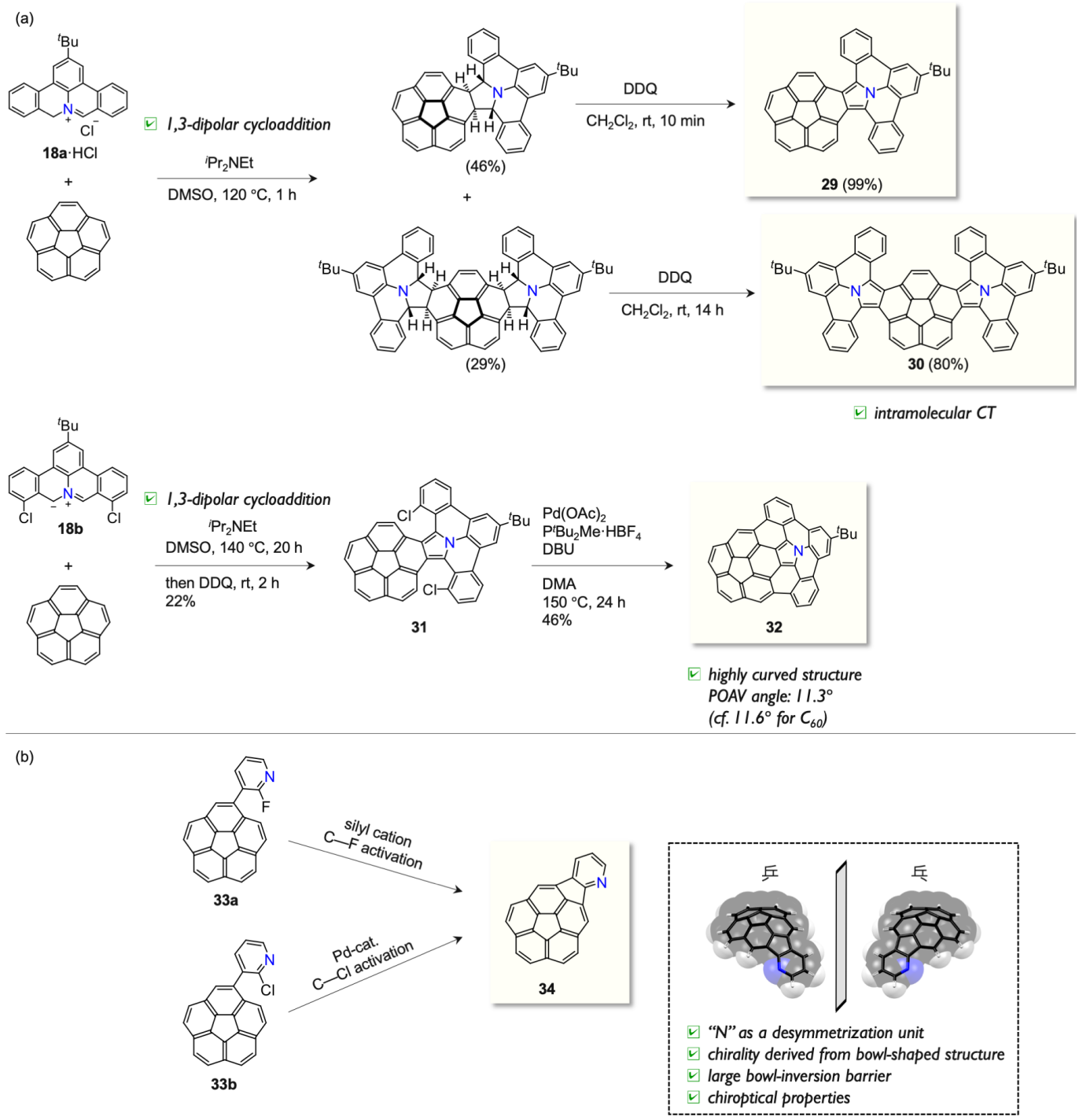

Scheme 4. Externally nitrogen doped corannulenes (a) Synthesis of pyrrole fused azacorannulenes and corannulene–azacorannulene hybrid (b) Chiral azaindenocorannulene and its chirality representations

In 2018, Siegel's group prepared C_1-symmetric azaindenocorannulene **34** from fluoropyridylcorannulene **33a** or chloropyridylcorannulene **33b** (Scheme 4b).[31] Azaindenocorannulene **34** possesses chirality derived from its bowl shaped geometry associated with the desymmetrized structure due to the doped nitrogen atom.

The bowl inversion barrier of *peri*-fused corannulene **34** is high enough to resolve the enantiomer. They investigated the chiroptical properties of **34** along with substituted indenocorannulene derivatives. Later, thiophene fused indenocorannulenes were prepared by similar methods utilizing palladium catalysis and their chiroptical properties were investigated.[32]

In 2019, the same group has synthesized a series of azaindenocorannulene imides **37**–**39** by a sequence including Suzuki–Miyaura coupling and palladium catalyzed C-H arylative cyclization for corannulene imide **36**, which was prepared by dehydration condensation of corannulene dicarboxylic anhydride **35** with (*S*)-heptan-2-amine (Scheme 5).[32] Among the resulting azaindenocorannulenes, **39** shows highly stable chirality, which is more inert configurationally than chiral biaryls, phosphenes, and [n]helicenes. In 2021, they further extended the chiral heteracorannulenes to thiophene fused system (**40**–**43**) (Figure 6).[33]

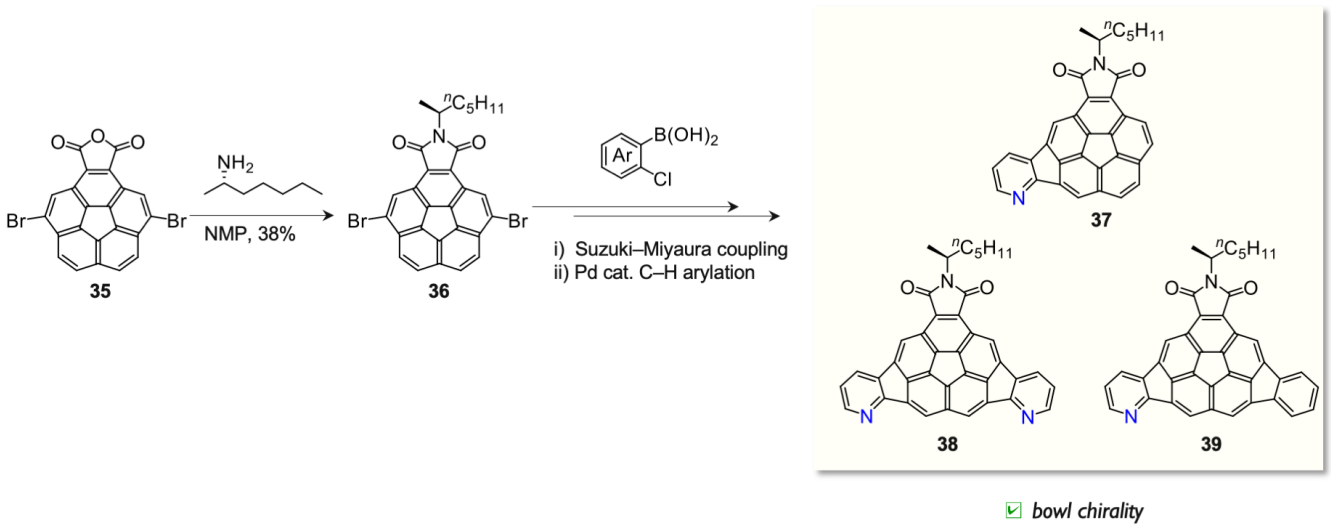

Scheme 5. Synthesis of chiral azaindenocorannulene imides

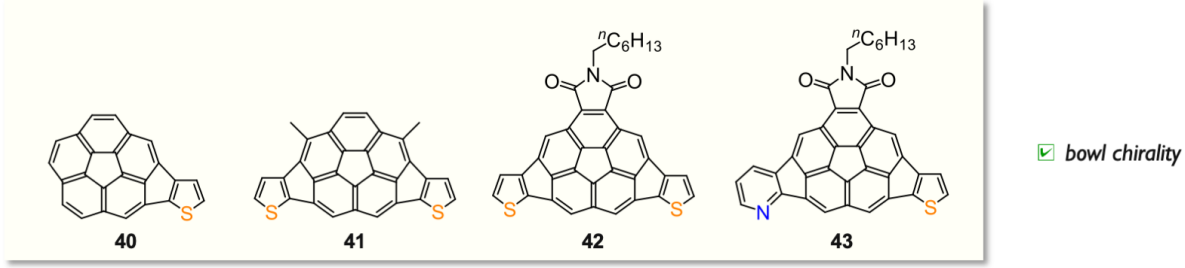

Figure 6. Thiophene fused corannulenes and corannulene imides

In 2018, Saha *et al*. synthesized diindole fused corannulene imide derivative **46** by Suzuki–Miyaura coupling of dibromocorannulene imide **44** with *o*-nitrobenzene boronic acid, followed by Cadogan type reductive cyclization of **45** using triphenylphosphine at 180 °C (Scheme 6).[34] Compared with corannulene

imide **47**, indole fused corannulene **46** exhibited perturbed properties such as smaller HOMO–LUMO gap and lower bowl-to-bowl inversion barrier.

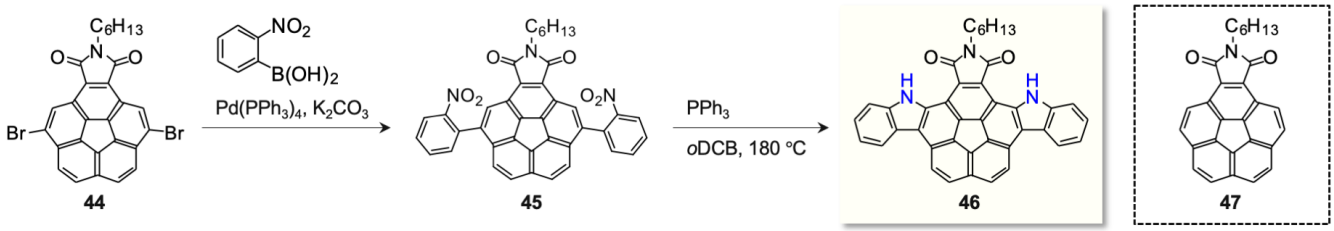

Scheme 6. Indole fused corannulene imide

Recently, Tanaka and co-workers have reported pentahalogenated corannulenes as useful intermediates for heteoatom incorporated corannulene (Scheme 7b).[35] They applied copper-mediated halogenation of *sym*-pentaborylcorannulene **55** to obtain *sym*-pentabromocorannulene **56** and *sym*-pentaiodocorannulene **57** in a preparative scale. Although *sym*-pentachlorocorannulene has been employed for various peripheral functionalization reactions because of its facile preparation from parent corannulene in one step, **56** and **57** had been unprecedented. Pentabromocorannulene **56** was used to synthesize pentaindolo- and pentakis(benzoindolo)corannulenes **59** and **61** by a reaction sequence including palladium catalyzed five-fold amination reaction with the corresponding chlorinated aromatic amine, palladium catalyzed intramolecular arylative cyclization under microwave irradiation, and *N*-methylation to improve the solubility.[36] The X-ray crystal structure of **59** has been revealed to be a multiple helicene type structure with *PPMPM* and *MMPMP* helical configurations. More in detail, the bowl chirality can be also defined because of the desymmetrized structure of the indole units. Therefore, associated with the bowl chirality *P* and *M*, the lowest energy form of **59** was represented as *M,PPMPM* and *P,MMPMP*, which was confirmed by the comparison of all the possible conformational isomers by DFT calculation with the aid of automated structure search program. The calculation predicted the most stable conformer of **61** to be *M,MMPMP* and *P,PPMPM*, but the energy differences between these and other conformers are rather small. Furthermore, all the possible interconversion network has been analyzed by calculating the transition states for helical inversion and bowl inversion, which illuminated the significant energy reduction due to cooperative helical and bowl inversion process in these quintuple azahelicene-corannulene hybrids as compared with single helicene-corannulene hybrid molecule.

Singly indole fused (**51**) and benzoindole fused corannulenes (**54**) were synthesized by the same protocol from iodocorannulene **48** (Scheme 7a). They exhibited bright blue emission with quantum yields of 0.17–0.25 in CH_2Cl_2. At low temperature, they exhibited long-lived (2.9–3.3 s) phosphorescence in the range of 500–750 nm.

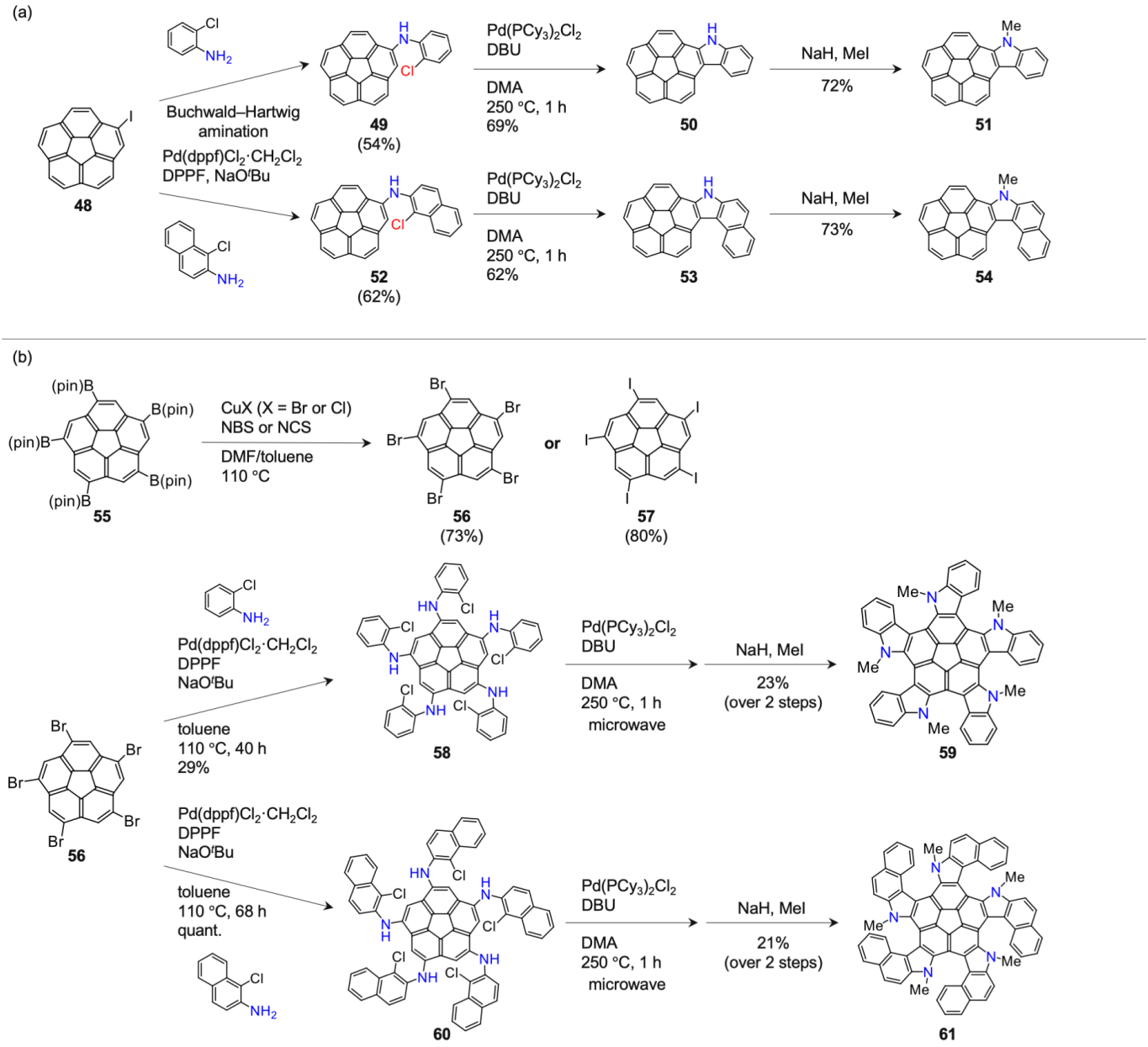

Scheme 7. Externally nitrogen doped corannulenes (a) monoindolocorannulenes (b) Pentaindolocorannulene and pentakis(benzoindolo)corannulene

Segawa and Itami reported an efficient method to obtain thiophene fused π-systems.[37] Arylethynyl-substituted corannulene **62** was heated in DMF in the presence of elemental sulfur to produce thiophene fused corannulene **63** in 99% yield (Scheme 8). This reaction was further applied to pentakis(arylethynyl)corannulene **64** and five-fold thienannulation resulted in the formation of thiophene-fused corannulene **65** in 20% yield.

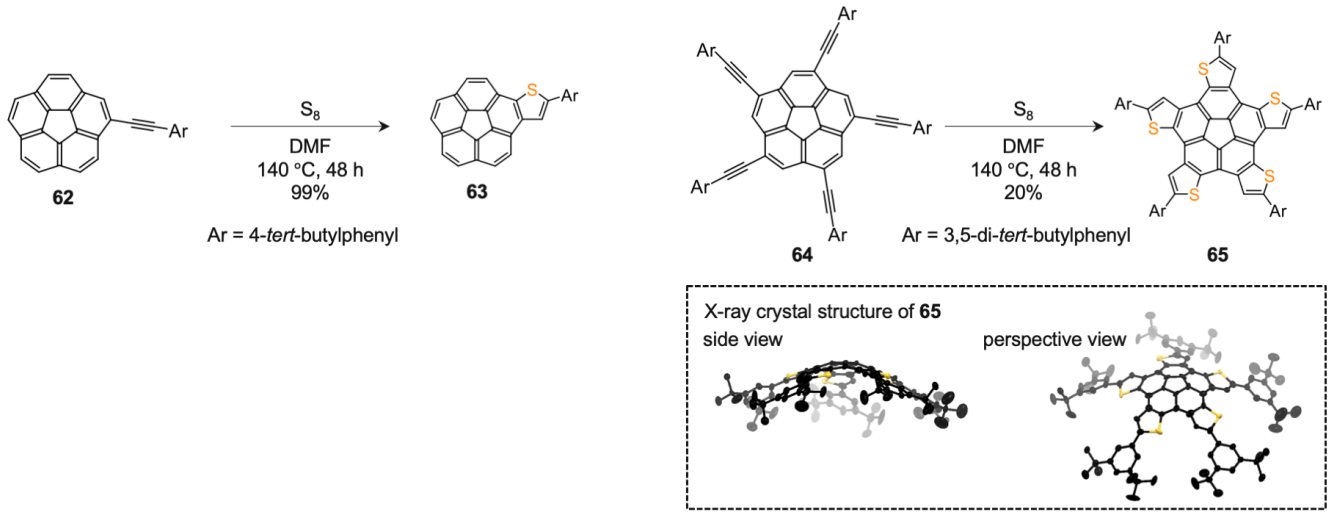

Scheme 8. Thienannulation reactions of arylethynyl-substituted corannulenes

3. SUMANENE

Sumanene ($C_{21}H_{12}$) is a C_{3v}-symmetric bowl shaped PAH, which consists of alternating benzene rings and cyclopentadiene rings around the central benzene ring (Figure 7).[8] The most significant difference from corannulene is the presence of the bridging sp^3-hybridized carbons. At this active benzylic position, stable sumanene cations, anions, radicals, and carbenes can be generated.[38] The bond length of the flank (b) is 1.548 Å which falls within the range of a typical C–C bond length. The bowl depth of sumanene (1.11 Å) is larger than that of corannulene (0.87 Å). The deeper bowl shaped geometry leads to a larger dipole moment (2.5 Debye) and a larger bowl-to-bowl inversion barrier (*ca*. 20 kcal mol^{-1}).

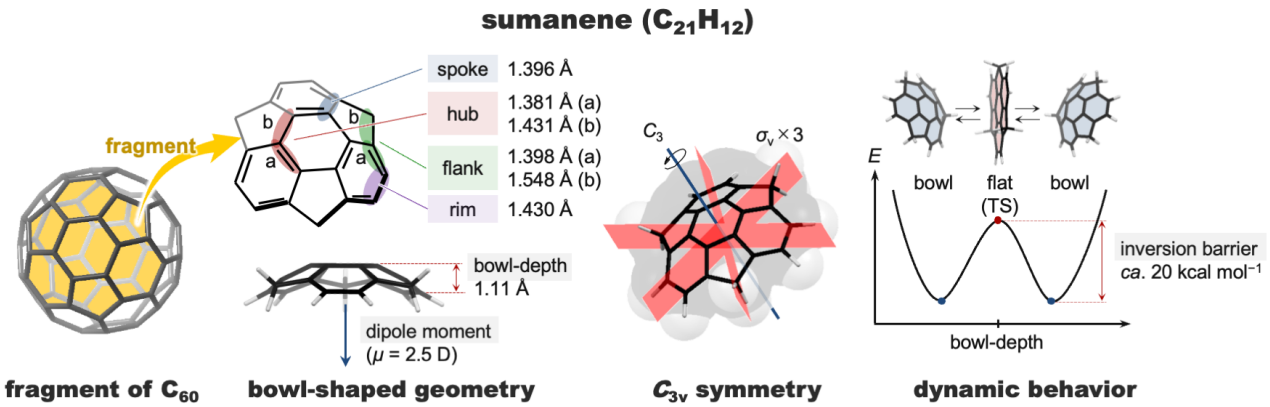

Figure 7. Structural relevance to C_{60}, the bowl shaped geometry, C_{3v} symmetry, and dynamic behavior of sumanene

Compared with corannulene, sumanene is more strained as seen in its larger POAV angle (9.0°), and its first synthesis was left behind over decades since the first preparation of corannulene. The synthesis of sumanene was first accomplished by short-step synthesis from 1,5-norbornadiene (**66**) (Scheme 9).[8] The

key to the success was to use sp^3-carbon based three-dimensional framework **68** as the precursor, whereas planar aromatic compounds such as triphenylene derivatives were used in previous attempts. In the successful approach, the imposed strain energy of sumanene was likely compensated by energy gain in oxidative aromatization of **68**.

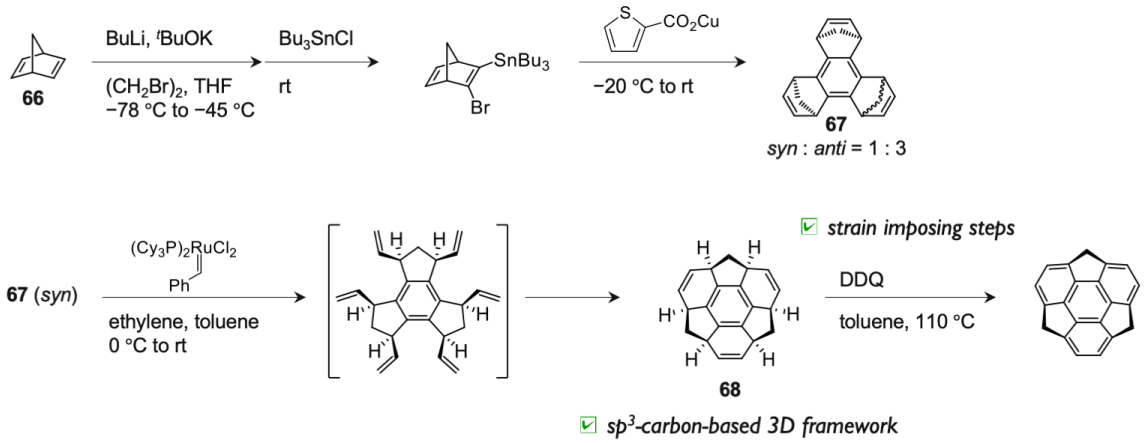

Scheme 9. The synthesis of sumanene

Recently, heteroatom doped congeners of sumanene have been actively explored.[39] The heteroatom doped sumanenes can be categorized into 1) sumanene congeners with heteroatoms at the rim positions and 2) sumanene congeners with heteroatoms at the benzylic positions (Figure 8). The former has been only exemplified by nitrogen doped sumanenes, while a variety of benzylic heteroatom doped sumanenes have been reported, which are referred to as heterasumanenes.

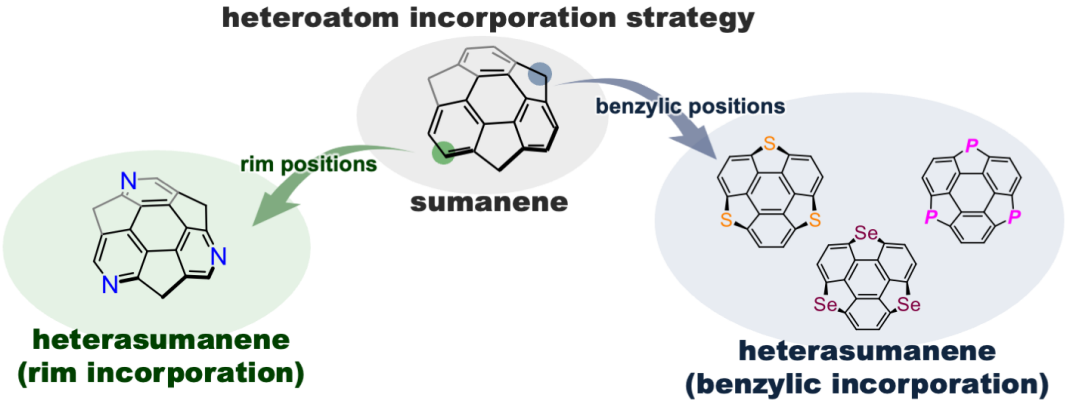

Figure 8. Two categories of heterasumanenes: rim incorporation and benzylic incorporation

3-1. HETEROATOM DOPED SUMANENE AT RIM POSITIONS

In 2012, Sakurai *et al*. reported the synthesis of triazasumanenes **75** and **76** having inherent chirality derived from bowl shaped structures (Scheme 10).[40] It was the first enantioselective synthesis of a chiral

azabuckybowl and their chiroptical properties were investigated. Nitrogen-doping modification led to more curved structures, deeper bowl depths, and higher bowl inversion energies compared with the pristine sumanene. Later, they transformed **75** into triaryltriazasumanenes **78** by palladium catalyzed cross coupling reactions without racemization.[41] Furthermore, they have successfully prepared the pristine triazasumanene **77** by desulfurization of **75** using organosilane as a mild hydride source.[42] Triazasumanene **77** was stable except under acidic conditions and the structures have been unambiguously determined by X-ray diffraction analysis. Notably, a helical columnar packing structure was observed for **77** in the enantiopure form, which was unprecedented for buckybowls.

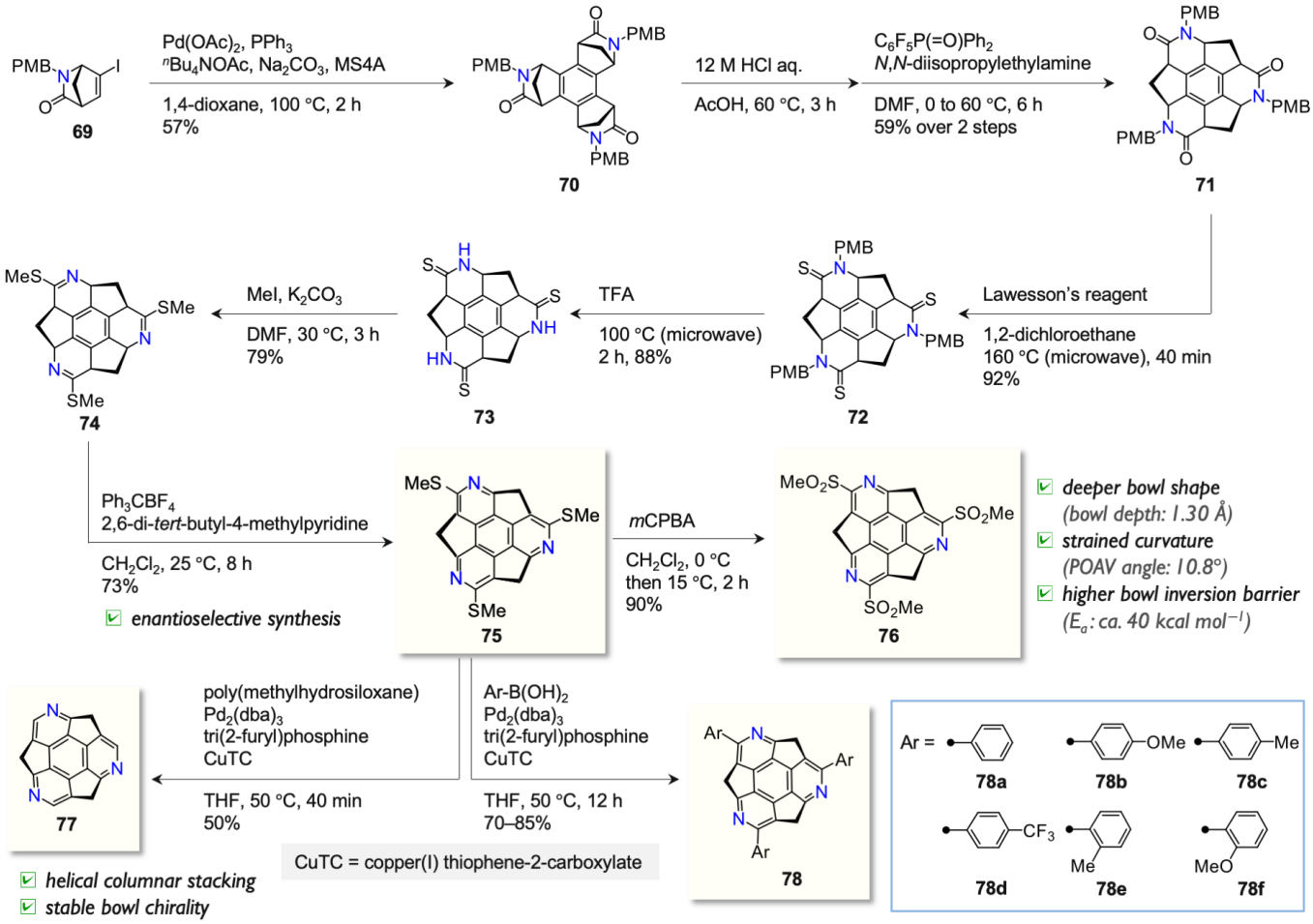

Scheme 10. Enantioselective synthesis of triazasumanenes

3-2. HETEROATOM DOPED SUMANENE AT BENZYLIC POSITIONS

Group 14 (Si, Ge, Sn), 15 (P), and 16 (S, Se, Te) elements have been doped at the benzylic positions of sumanene. As a pioneering work, trithiasumanene **81** was synthesized from thiophene trimer **79** via intermediates **80a**,**b** by Otsubo *et al*. (Scheme 11a).[43] Although **31** was the first bowl shaped heteroaromatic compound, the harsh reaction conditions involving FVP resulted in a low total yield of less than 5% on a milligram scale. In 2014, Shao *et al*. reported the non-pyrolytic synthesis of trithiasumanene **83a** and

triselenasumanene **84a** in short steps from less expensive triphenylene derivative **82a** on a multigram scale (Scheme 11b).[44] Due to the significantly longer bond length of C–Se (1.93 Å) than that of C–S (1.80 Å), triselenasumanene **84a** takes a shallower bowl shaped structure compared with trithiasumanene **83a**, leading to the bowl depths of **84a** (0.47 Å) and **83a** (0.70 Å). In 2016, the same group prepared tritellurasumanenes **85a**,**b**.[45] Tritellurasumanene **85b** adopts an almost flat structure in the solid-state, reflecting a much longer bond length of C–Te (2.10 Å). A variety of heterasumanenes including these elements have been reported in a similar way.[46]

In 2009, Kawashima and Kobayashi *et al*. developed intramolecular sila-Friedel–Crafts reaction and applied it for the construction of trisilasumanene **88** (Scheme 11c).[47] X-Ray diffraction analysis revealed that the main framework of **88** was almost planar and the C–Si bond lengths are in the range of 1.88-1.92 Å. Weak absorption in the longer wavelength region of **88** suggested the existence of σ^*–π^* conjugation on the doped silicon atoms.

In 2017, Furukawa *et al*. successfully synthesized triphosphasumanene trisulfide ***syn*-89** and ***anti*-89** (Scheme 11d).[48] Notably in ***syn*-89**, the π-surface with the sulfur atoms is negatively polarized whereas that with the phenyl groups is positively polarized. Thus, ***syn*-89** possesses large out-of-plane anisotropy, resulting in a large dipole moment (12.0 Debye) compared with the previously reported anisotropic molecules. In addition, it was revealed that ***syn*-89** strongly adsorbed on the Au(III) surface using three sulfur atoms, which is another consequence of out-of-plane anisotropy.

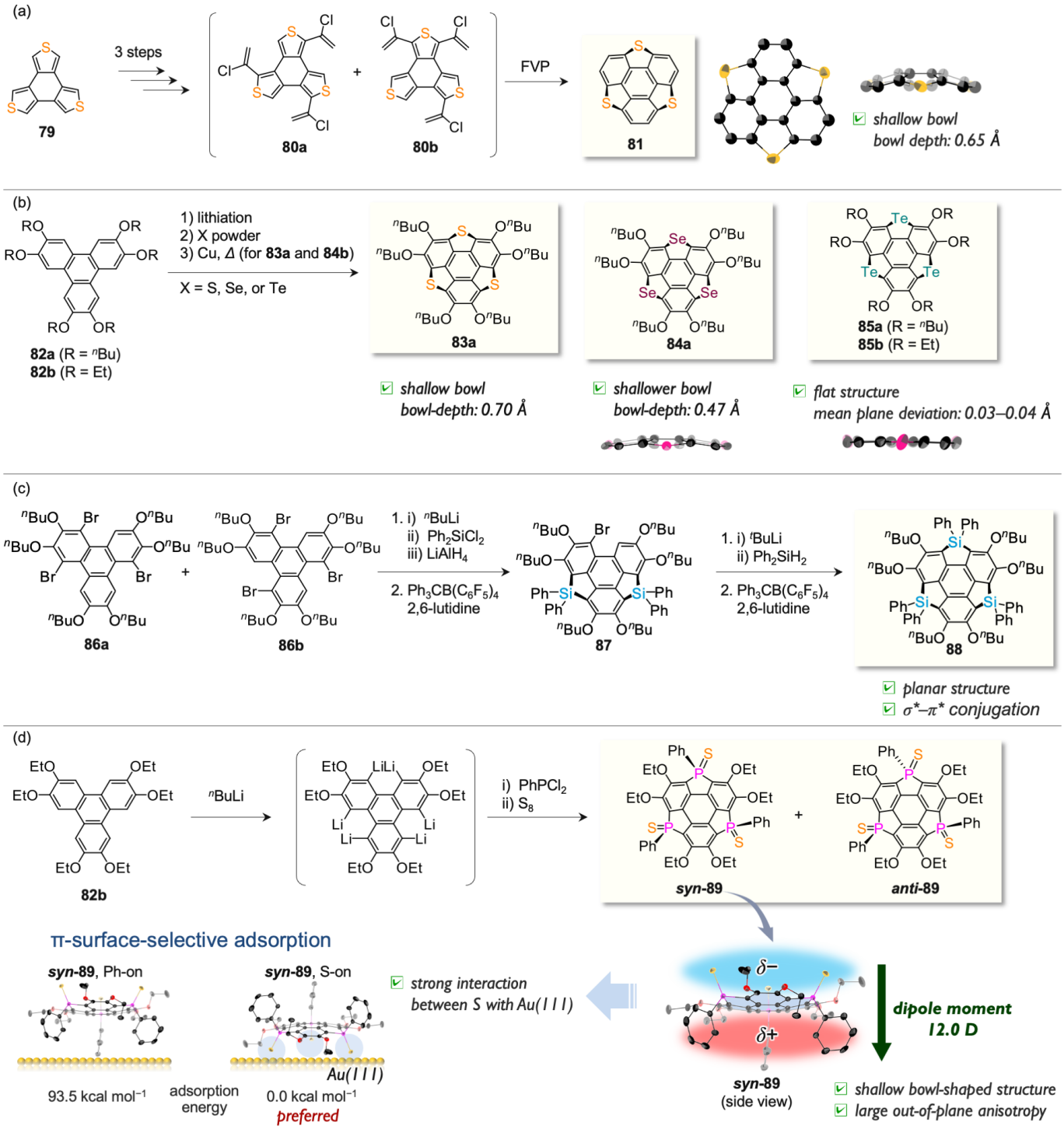

Scheme 11. Synthesis of (a) trithiasumanene, (b) chalcogen doped sumanenes, (c) trisilasumanene by sila-Friedel–Crafts reaction, and (d) triphosphasumanene trisulfides

In spite of the development of above-mentioned heterasumanenes, azasumanenes with doped nitrogen atom at the benzylic positions was thought to be difficult to synthesize because of the shorter C–N bond length and larger bowl strain energy. Tanaka and Osuka envisioned the synthesis of tribenzotriazasumanene by

fold-in type fusion of **90** (Scheme 12a). However, the oxidation using $FeCl_3$ gave undesired fused product **91** while bromination followed by reductive fusion afforded incompletely fused product **93**.[49]

Very recently, Shao's group synthesized nitrogen doped sumanenes at the benzylic position (Scheme 12b).[50] First, the pivotal intermediate **95a**,**b** was prepared by iodination of **82a**, followed by Buchwald–Hartwig amination. Then, after the subsequent reaction(s), azadithia- (**96a**,**b**), azadiselena- (**97a**,**b**), and azaditellura-sumanene (**98a**,**b**) were synthesized. These are the first examples of heterasumanene with the embedded nitrogen at the benzylic position. Crystallographic analysis revealed that the bowl depth became shallower in going from **96b** to **98b**. Interestingly, azachalcogenasumanenes **97b** and **98b** underwent ring reconstruction via atom transfer under acidic conditions, while such a reconstruction reaction was very slow in **96b**, indicating that the conversion rate and relative product ratio depend on the type of chalcogen atom.

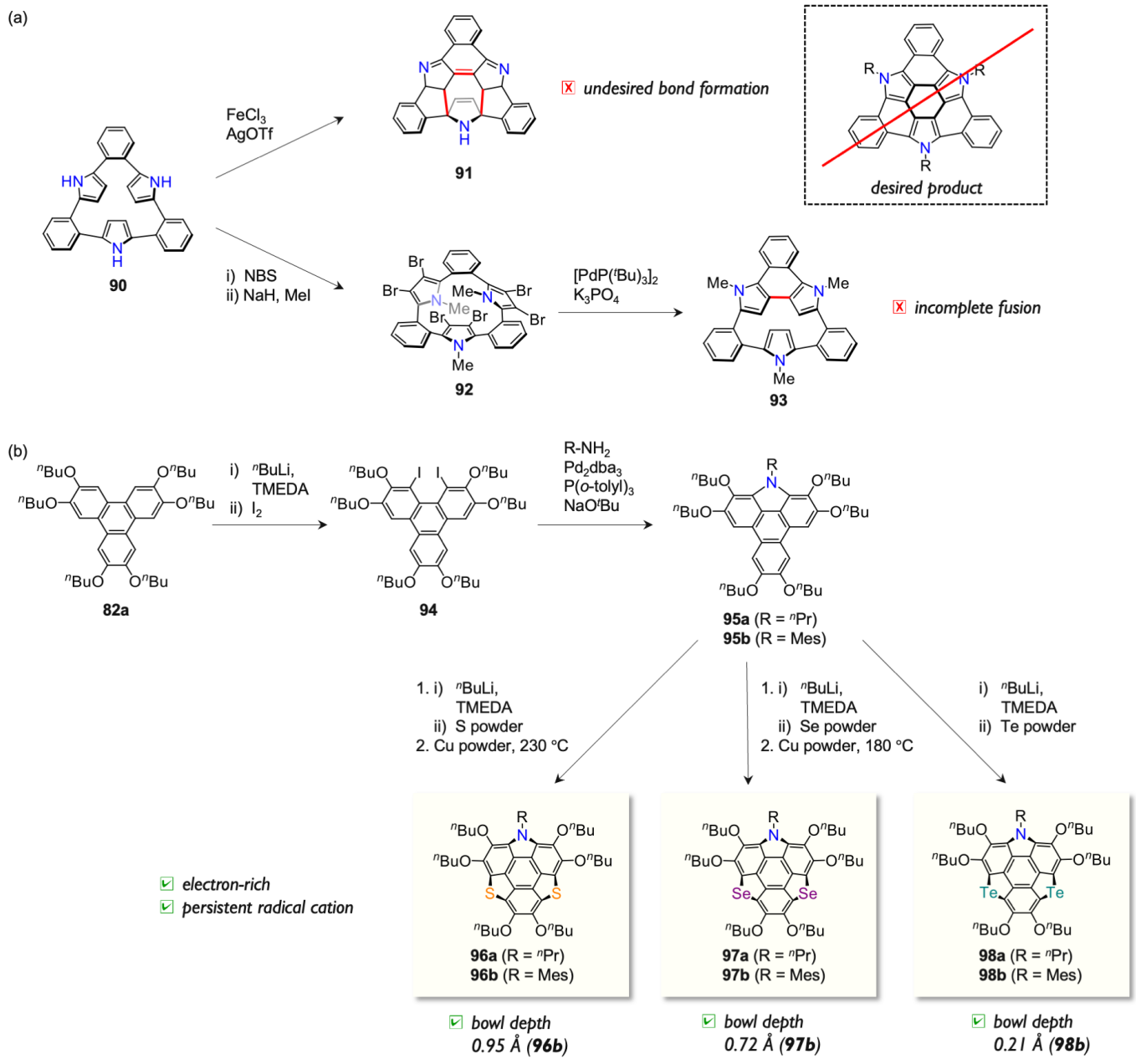

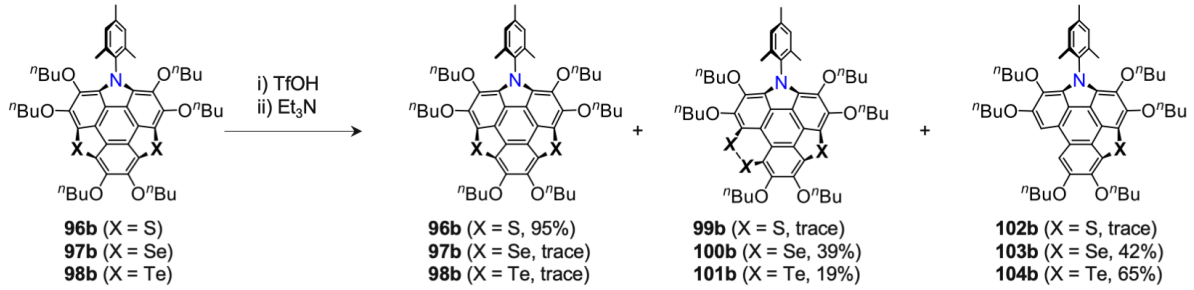

Scheme 12. (a) Attempts to prepare tribenzotriazasumanene and (b) recent successful synthesis of monoazadichalcogenasumanenes

In 2012, Saito *et al*. synthesized trisilasumanene **108** bearing no substituents on the peripheral benzene rings from the pristine triphenylene **105** by repetitive lithiation and silylation via **106** and **107** (Scheme 13a).[51] Moreover, they applied the repetitive two step reaction sequences to the synthesis of trigermasumanene **112** from triphenylene **105** via **109** and **110** (Scheme 13b). They also attempted to prepare tristannasumanene in a similar way, but it was not successful since the undesired C—Sn bond cleavage occurred competitively to the desired lithiation at the bay regions of triphenylene skeleton, leading to the incompletely stannylated products **114**, **115**, and **116** in low yields (Scheme 13c). Similar trisila and trigermasumanenes were also synthesized by rhodium catalyzed cyclodehydrogenation reactions by Tan and Xu in 2017.[52]

In 2010, Saito *et al*. reported the synthesis of heterasumanene including three different heteroatom functionalities, namely, **120a** (S, Si, Si) and **120b** (S, Si, Sn), from triphenylenothiophene **117** (Scheme 13d).[53]

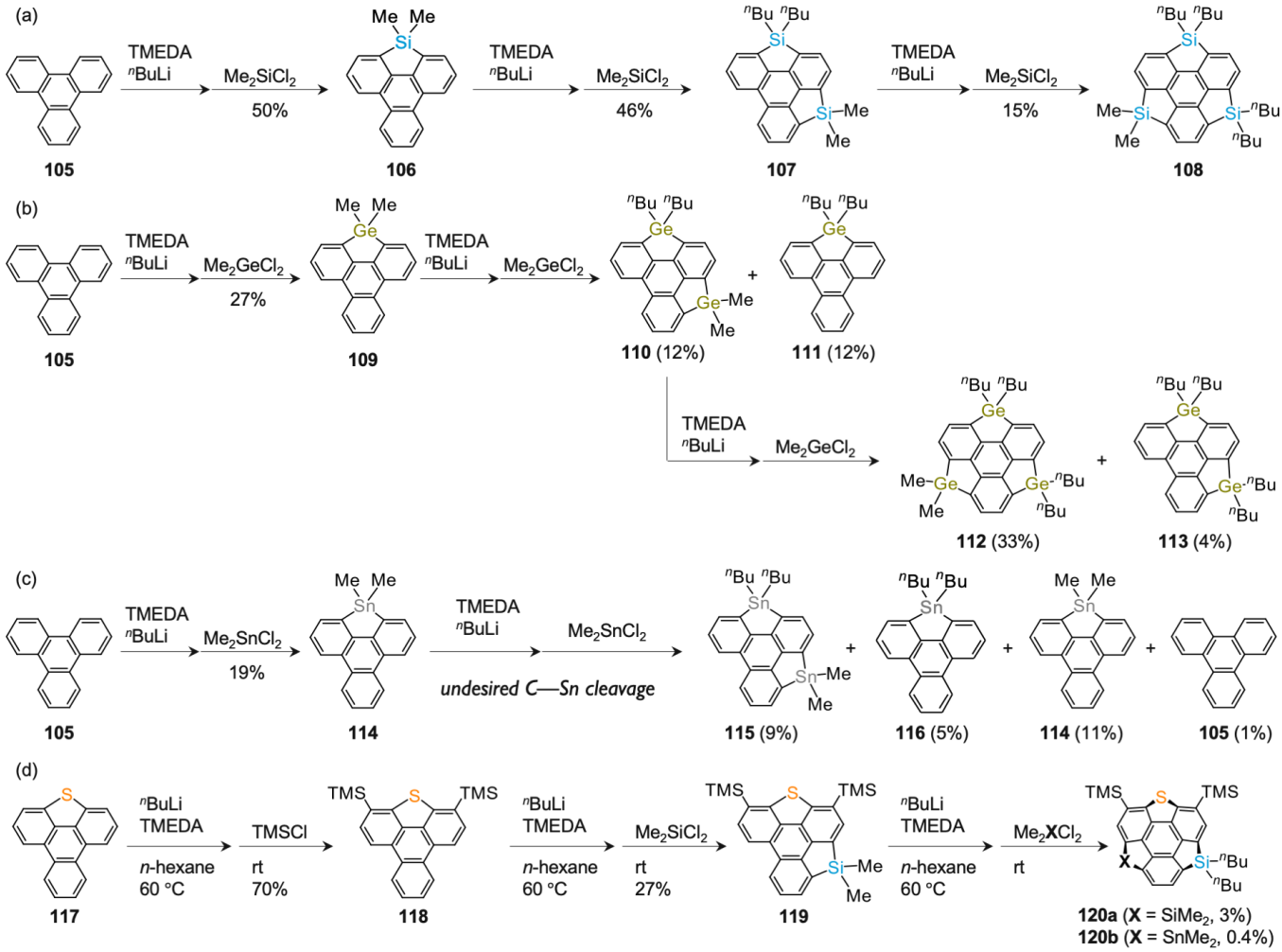

Scheme 13. Synthesis of (a) trisila and (b) trigermasumanenes (c) An attempt to synthesize tristannasumanene (d) Synthesis of heterasumanene including three different heteroatoms

1.5. OTHER HETEROATOM DOPED BOWL SHAPED PAH

In this section, we introduce several heteroatom embedded PAHs reported during 2010–2022.

In 2013, Stępień *et al*. synthesized bowl shaped [3]chrysaorole **122a** from the cyclic precursor **121a** using nickel catalyzed reductive coupling conditions (Scheme 14).[54] Generally, the synthesis of bowl shaped compounds relies on a straightforward methodology in which the bowl is constructed from the center (hub) to the periphery (rim). Unlike the conventional approach, Stępień proposed a new methodology called "fold-in," in which a macrocyclic precursor containing the complete rim is prepared first, and then, the central hub of the bowl is constructed afterward. Later in 2021, Miao's group synthesized benzo fused analogue **122b** from cyclic precursor **121b** by employing the "fold-in" type oxidation.[55]

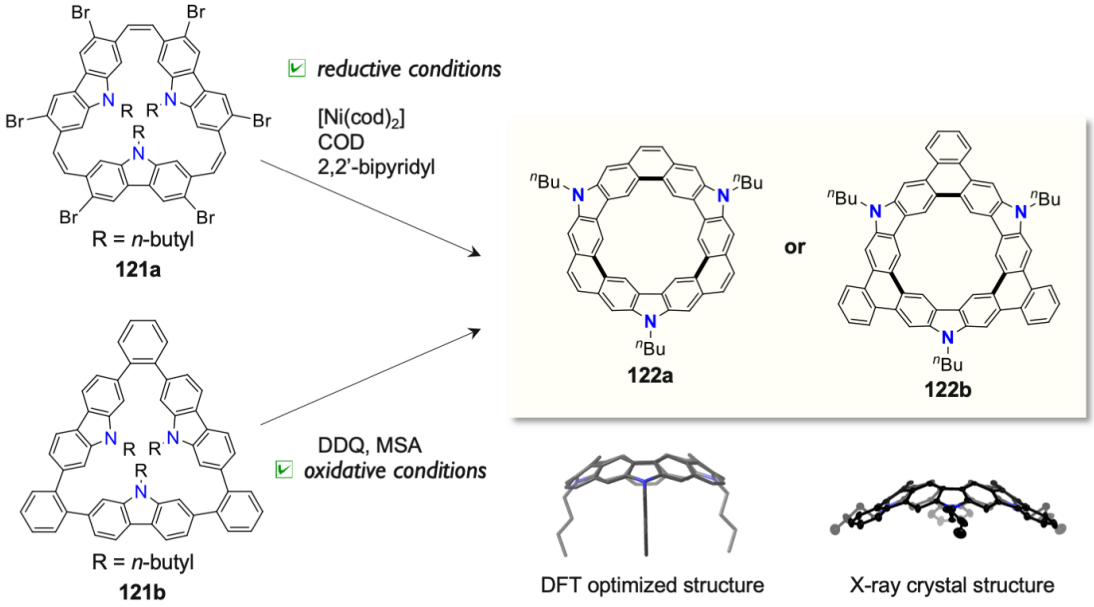

Scheme 14. "Fold-in" type synthesis toward bowl shaped cyclic PAHs

In 2016, Higashibayashi *et al*. reported hydrazine embedded azabuckybowl **125** by N—N linking oxidation of cyclobicarbazole **124** by DDQ (Scheme 15a).[56] Azabuckybowl **125** was oxidized to its radicalcation (**125**$^{\bullet+}\cdot SbF_6^-$) and dication salts (**125**$^{2+}\cdot 2SbF_6^-$) by controlling the equivalents of the oxidant, nitrosonium hexafluoroantimonate. Interestingly, the azabuckybowl takes different structures depending on its oxidation state; bowl shaped for monocation **125**$^{\bullet+}$ and planar for dication **125**$^{2+}$. For the neutral species **125**, a bowl shaped structure was calculated as the most stable conformer, while a twist-shaped structure was observed in the solid-state as a meta-stable conformer.

Recently, the group of Seki and Tanaka has reported the synthesis and properties of hydrazine embedded benzannulated pyracylenes **128a**,**b**, which were obtained by oxidative N—N linking reaction of cyclophane type precursors **126a**,**b** using potassium *tert*-butoxide under aerial conditions.[57] The reaction also provided a side-product **127**, in which the N—C bond formation took place associated with quenching reaction with oxygen or water. Diazapyracylene **128a** displayed a well ordered π-stacking structure with high carrier mobility in the solid state. The estimated carrier mobility was proved to be much better than the reference molecule, dibenzoullazine **129**, which showed a similar π-stacking structure in the solid-state. In addition, ^{1}H NMR and UV-vis absorption spectra of **128a** indicate the decent contribution of 12π antiaromaticity by comparing with **129**, although its contribution is weak and local 6π aromatic conjugation works as a dominant contribution (Scheme 15b). The radical cation of **128a** was cleanly observable by an addition of tris(4-bromophenyl)ammoniumyl hexachloroantimonate in solution but its dication was unlikely stable.

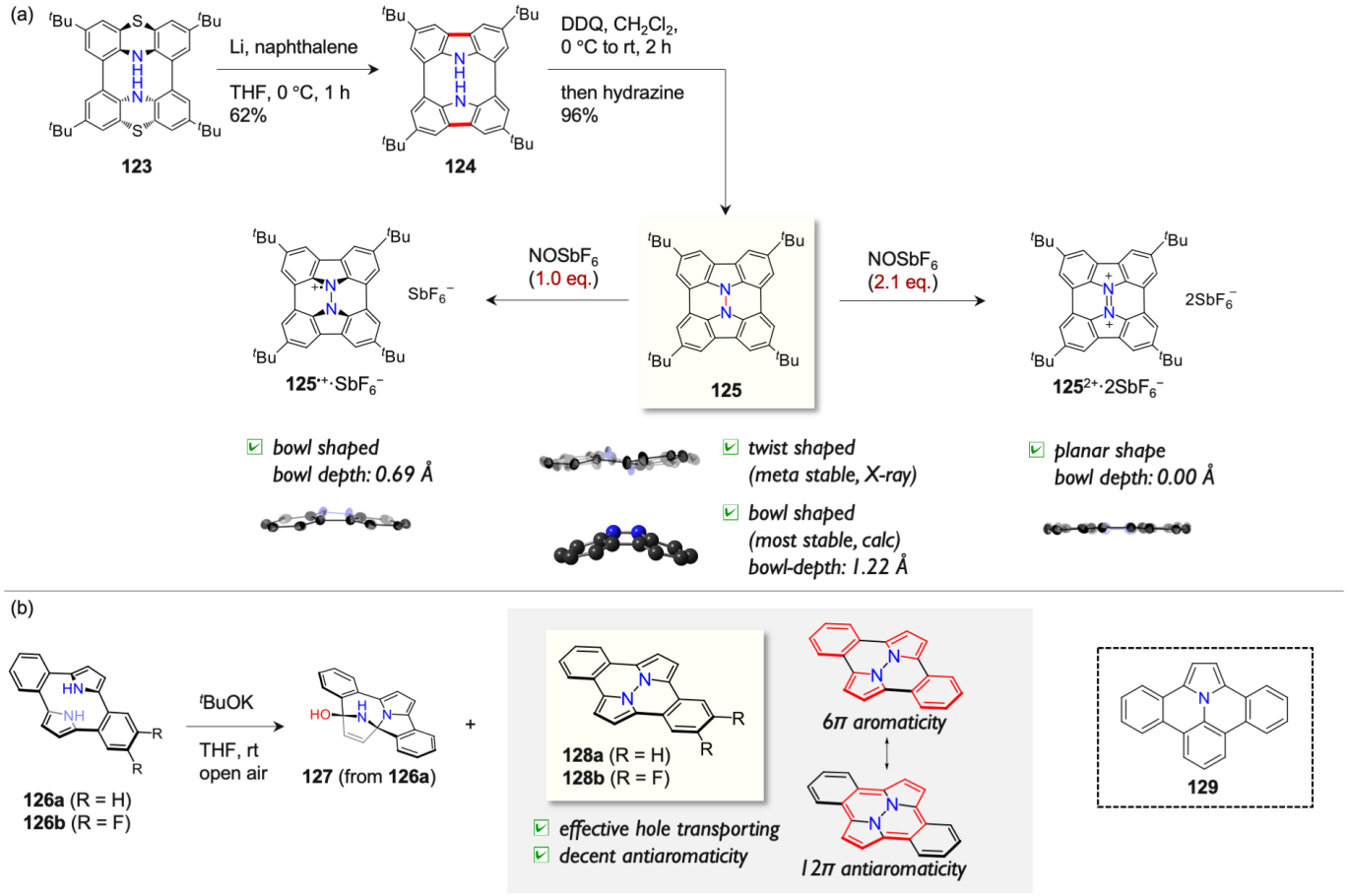

Scheme 15. (a) Redox-dependent transformation of the geometry of hydrazine embedded buckybowl (b) Synthesis of dibenzodiazapyracylene and a decent contribution of dual aromaticity

In 2018, Gryko *et al*. have prepared pyrrolo[3,2-*b*]pyrrole based azabuckybowl **134a** using on-surface conditions in the final step (Scheme 16).[58] The bowl shaped molecule **134a** contains two central pentagons confined between the two adjacent heptagons, which is called inversed Stone–Thrower–Wales (ISTW) topology. The topology is found in defects in graphene and is difficult to obtain experimentally. Later, the same group have reported the synthesis of the *tert*-butyl–substituted analogue **134b** by an only in-solution approach over 4 steps from **131**–**133**.[59]

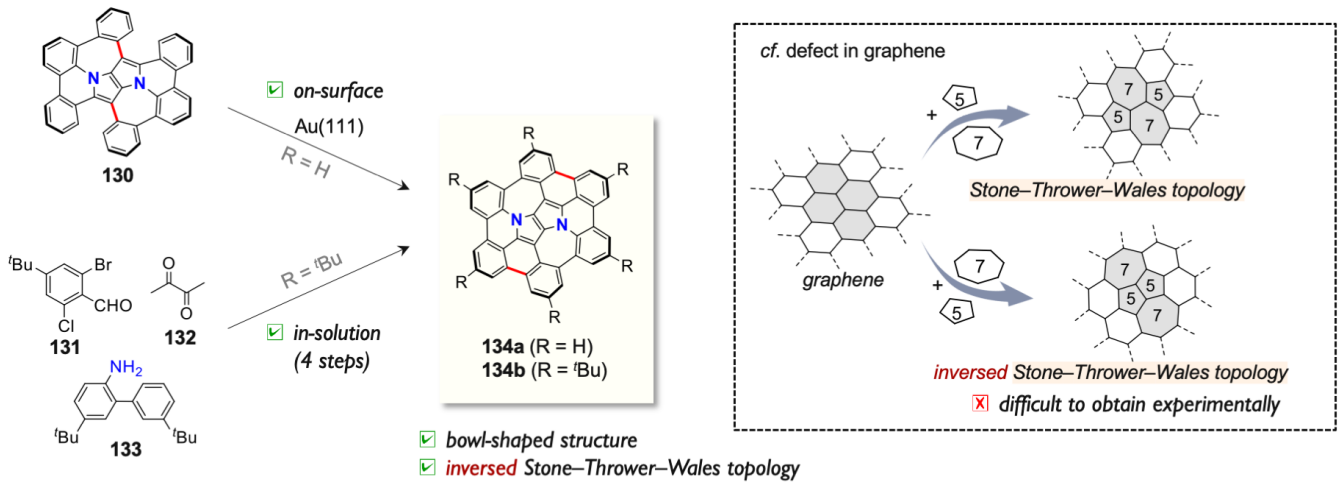

Scheme 16. Pyrrolopyrrole-based azabuckybowl bearing inversed Stone–Thrower–Wales topology

5. HEXAPYRROLOHEXAAZACORONENE

Among nitrogen doped PAHs, hexapyrrolohexaazacoronene (HPHAC) has been extensively studied because of the analogy to hexa-*peri*-hexabenzocoronene in terms of its structure and synthetic method. The first report of HPHAC in 2003 only described its MALDI-TOF-MS results.[60] Later in 2007, Müllen's group have successfully synthesized HPHACs **137b**,**c** from the corresponding hexapyrrolobenzenes upon oxidation with $FeCl_3$ in dichloromethane/nitromethane and subsequent neutralization (Scheme 17a). Essentially the same method has been employed to produce HPHAC analogs afterward. They also conducted chemical oxidation of **137c** and isolated its dication species **137c**$^{2+}$. The neutral and dication species have been fully characterized by X-ray analysis and UV/Vis spectroscopy.[61] Very recently, dodecaethyl-substituted HPHAC **137d** was synthesized by Takase and Uno.[62]

After that report, several groups developed the chemistry of HPHAC through structural modification such as the peripheral expansion of the macrocyclic circuit, core-expansion, and peripheral substitution/π-extension (Scheme 17b).

Gońka and Stępień *et al*. have synthesized **142** and **144** containing sp^3-carbon bridge(s) at the periphery.[63] The bridge was introduced first by condensation of hexapyrrolobenzene **138** with *p*-nitrobenzaldehyde and subsequent oxidation with DDQ afforded the products. Notably, **139** served as an efficient NIR chromophore whose absorption band reached 2400 nm when oxidized up to trication. In addition, the biradicaloid character of **144**$^{2+}$ was suggested by the low-temperature ^{1}H NMR spectrum and DFT calculation.

In 2019, Takase and Uno *et al*. synthesized monocationic species **146a**,**b**$^{+}$ and their corresponding trication **146a**,**b**$^{3+}$ bearing a peripheral sp^2-carbon bridge.[64] In this case, the bridge was introduced after partial fusion of hexapyrrolobenzene by Vilsmeier-Haack reaction. The ^{1}H NMR, NICS, and ACID analysis revealed

that the monocation exhibited global 24π antiaromaticity while the trication exhibited global 22π aromaticity. This is the first set of Hückel antiaromatic monocation and Hückel aromatic trication pairs in HPHAC.

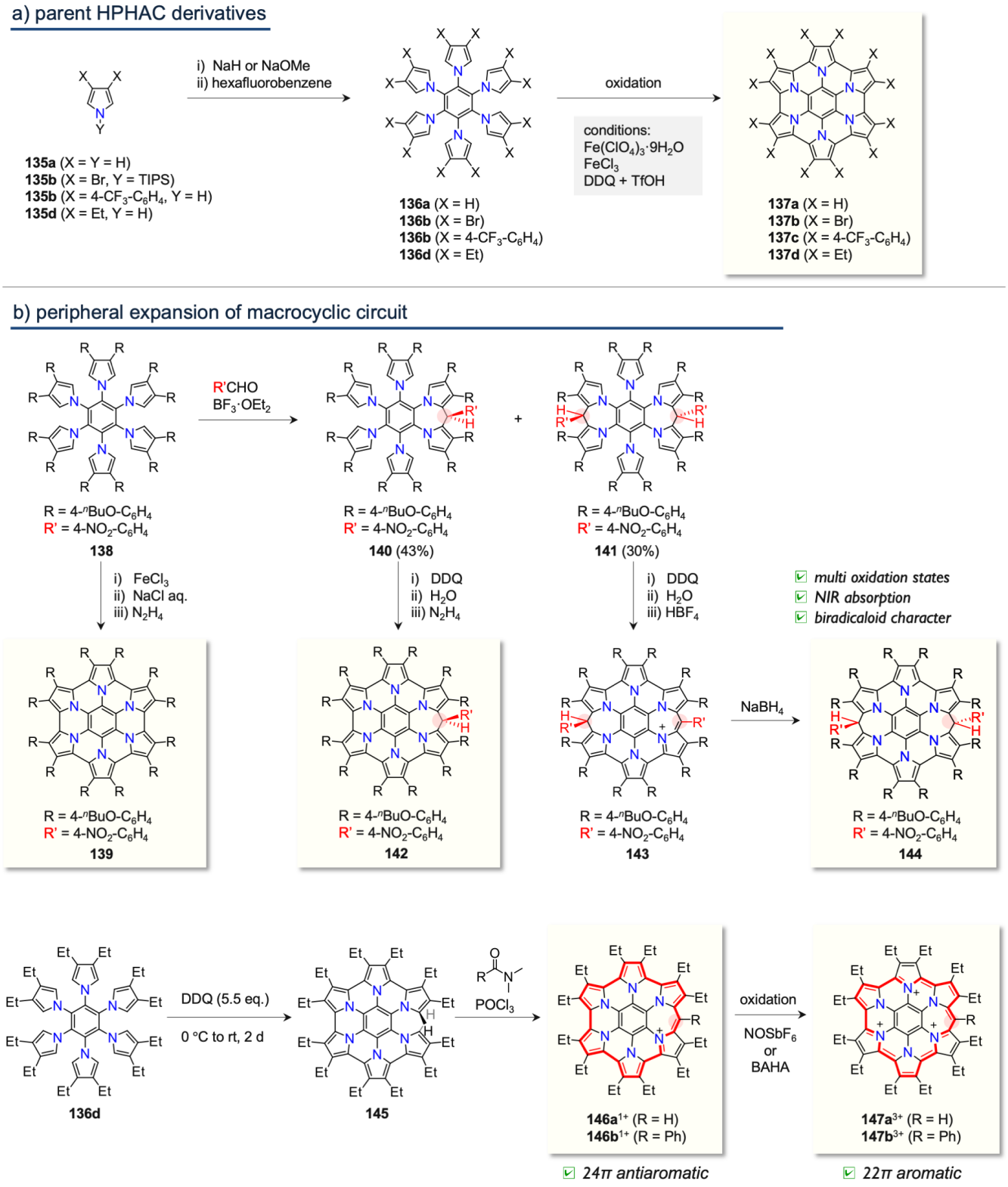

Scheme 17. HPHAC and its development

Stępień *et al*. reported radially π-expanded HPHAC **148** bearing six naphthalene monoimide motifs (Figure 9).[65] Owing to the electron-withdrawing imide moieties, **148** can accommodate up to 10 electrons, resulting in small electronic band gaps and panchromatic absorption spectra. As a similar motif, Takase, Kobayashi, and Uno *et al*. reported radially acenaphthylene fused HPHAC **149** and their double concave structure.[66] They elucidated the association behavior of **149** with C_{60} by taking advantage of the electron-rich bowl shaped surfaces.

Core-expanded azacoronene analog **150** has been successfully synthesized in just two steps from commercially available octafluoronaphthalene by Takase and Uno.[67] In the crystal structure, **150** took longitudinally twisted geometry. Despite such non-planarity, its dication $\mathbf{150}^{2+}$ exhibited global Hückel 30π aromaticity along the peripheral circuit. The twist-to-twist inversion barrier was estimated to be 5.9 kcal/mol via a saddle shaped transition state. Notably, the benzene-based analogue **151** has not been synthesized yet probably due to the severe distortion.

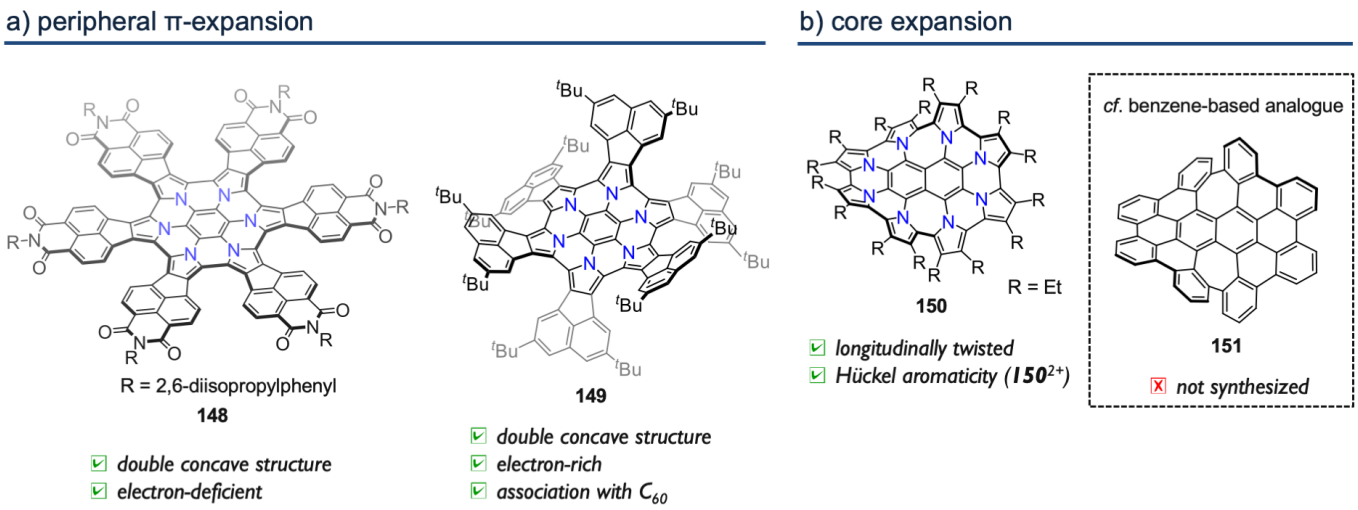

Figure 9. π-Expanded HPHAC analogues

6. HETEROCIRCULENE

[n]Circulene is a polycyclic aromatic hydrocarbon with n-sided carbon framework at the center (Figure 10). Corannulene is indeed classified as [5]circulene, while [6]circulene is known as coronene.[68] Other [n]circulenes reported until 2021 are quadrannulene (n = 4; only benzannulated one),[69] pleidannulene (n = 7),[70] and [8]circulene (n = 8; only peripherally substituted ones).[71] They take bowl shaped (n = 4, 5), planar (n = 6), and saddle shaped structures (n > 6) depending on the size of the central n-membered ring. Recently, their heteroatom incorporated variants have also been intensively studied to reveal their perturbed electronic properties and structural distortion originating from the embedded heteroatom(s). In the following sections,

we pick up some selected examples of heteroatom embedded [n]circulenes including hetero[8]circulenes, hetero[9]circulene, and hetero[10]circulene mainly focusing on their structures.

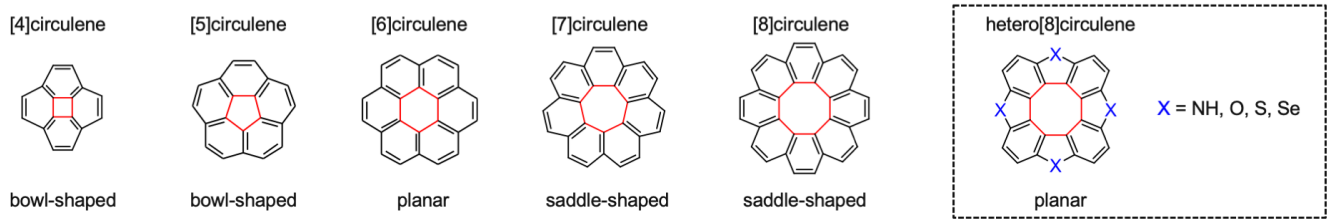

Figure 10. [n]Circulenes and hetero[8]circulenes

6-1. HETERO[8]CIRCULENE

Among hetero[n]circulenes, hetero[8]circulenes have been actively studied by several research groups. A variety of heteroatoms including nitrogen, oxygen, sulfur, and selenium have been embedded onto the [8]circulene skeleton, which was recently reviewed by several groups.[72]

Pittelkow's group has explored aza[8]circulenes using 3,6-dimethoxycarbazole derivatives as the common starting materials. The first hetero[8]circulene bearing nitrogen atom was synthesized in 2013 (Scheme 18a).[73] Azatrioxa[8]circulenes **153a** and **154a** were synthesized by acidic condensation of quinone derivative or naphthoquinone with 3,6-dihydroxycarbazole derivatives **152a** in 65% and 75% yields, respectively. X-Ray crystallographic analysis revealed that **153a** and **154a** took planar geometry unlike the pristine carbonous [8]circulenes which took saddle shaped structures.

Pittelkow *et al*. also synthesized diazadioxa[8]circulenes by acid mediated dimerization of 3,6-dihydroxycarbazole derivatives **152a**,**b** presumably via a tetrahydroxy form **155**. They investigated the antiaromaticity of the central 8π cyclooctatetraene moieties in **156a**,**b**.[74] The positive NICS(0) and NICS(1)^{zz} values (+8.6 and +20.9 ppm, respectively) were shown as a sign of antiaromaticity.

Recently, Pittelkow *et al.* has reported a rational synthetic approach to hetero[8]circulene **162** via ring closure of hetero[7]helicene **160** using tetrabutylammonium iodide (TBAI) and BCl_3 followed by an addition of *o*-chloranil and $BF_3{\cdot}OEt_2$ (Scheme 18b).[75] This is the first study describing hetero[8]circulene including three different heteroatoms. Meanwhile, treatment of [7]helicene **160** with *o*-chloranil and $BF_3{\cdot}OEt_2$ yielded *quasi*-diazathia[8]circulene **161** which contains seven surrounding (hetero)aromatic units around the central eight-membered ring. Due to the steric congestion between the two methoxy groups, the structure was heavily twisted. Similar *quasi*-aza[8]circulenes were reported by Tanaka and Osuka (Scheme 18c).[76] They reported selective syntheses of *quasi*-aza[8]circulenes **165a** and aza[7]helicenes **164a–c** under different oxidation conditions from the *ortho*-phenylene bridged indole-pyrrole-indole precursors **163a–c**. The substituents attached on the indole moiety play a crucial role. Interestingly, while dimethyl- and dichloro-substituted precursors only gave aza[7]helicenes upon oxidation with PIFA, the same oxidation

of more sterically demanding methoxy-substituted one **163d** furnished *quasi*-aza[8]circulene **165d** exclusively. Demethylation of **165d** with BBr_3 gave triazaoxa[8]circulene **167** in a good yield via a dihydroxy form **166**. The structure of **167** was revealed to be completely planar, and it exhibited emission around 449 nm with high quantum yield (0.72) in DMSO.

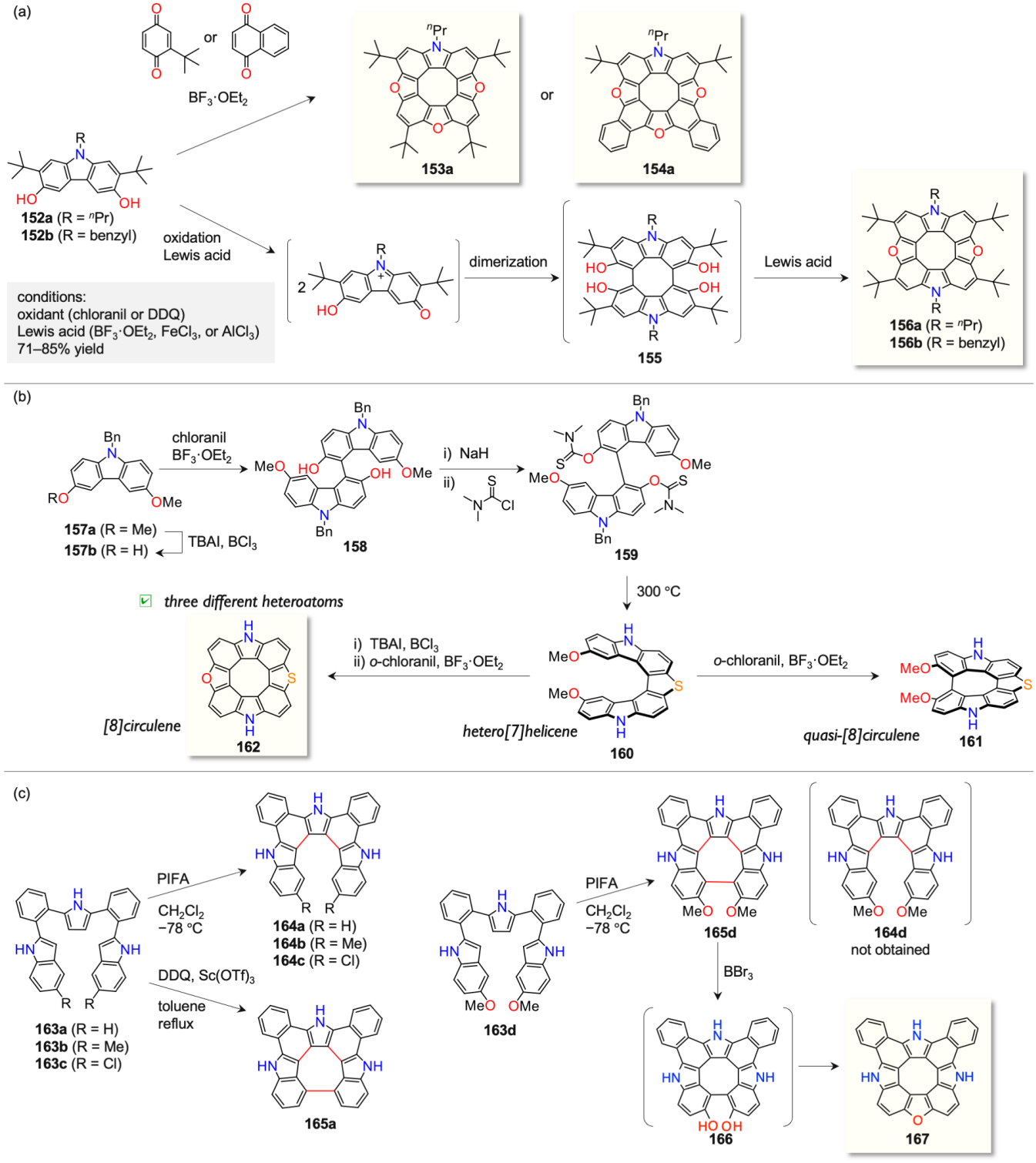

Scheme 18. Rational synthesis of hetero[8]circulenes and *quasi*-hetero[8]circulenes including heteroatoms (a) N and O, (b) N, O, and S, and (c) N and O

In 2015, Tanaka and co-workers synthesized the first tetraaza[8]circulene **169** by fold-in type oxidation of cyclic *ortho*-phenylene bridged tetrapyrrole **168** as the key step (Scheme 19).[77] The structure was completely planar as revealed by X-ray diffraction analysis. Notably, the external NH moieties were involved in a hydrogen bonding network with solvent molecules, which endowed the molecule with good solubility in THF, acetone, and DMSO. The antiaromatic character of the central cyclooctatetraene motif in **169** is weakened probably due to the longer C–C bonds around the 8-membered ring.

Tetraaza[8]circulene **169** exhibits sharp absorption and efficient fluorescence with its Stokes shift of only 150 cm^{-1}. *N*-Alkylated tetraaza[8]circulenes **170a**–**d** were prepared and their perturbed optical and electrochemical properties were investigated in detail.[78] Upon introduction of *N*-substituents, UV-vis absorption and fluorescence spectra were red-shifted since the structures were deviated from the original planar structure due to the increased steric congestion around nitrogen atoms.

Recently, an improved synthetic method has been developed to access to tetraaza[8]circulenes **171a**–**c** bearing substituents at the benzo scaffolds using commercially available 1,2-dibromobenzene derivatives.[79] Tetraaza[8]circulenes **171a**–**c** shows perturbed electronic properties depending on the substituents.

Another synthetic route toward quadruply *N*-substituted tetraaza[8]circulene from diazadithia[8]circulenes **175a**,**b** was reported, in which nucleophilic aromatic substitution reaction of diazadithia[8]circulene S,S'-tetraoxide **174** was a key reaction.[80] The structures of tetraaza[8]circulene **175a**,**b** bearing *N*-aryl substituents are slightly twisted as compared with pristine tetraaza[8]circulene **169**. In addition, **175a**,**b** can be easily oxidized to afford highly stable radical cations and their magnetic properties were elucidated by ESR and SQUID measurements. A similar substitution protocol has been employed to give diazadimethano[8]circulene **176** using diphenylmethane as the nucleophile.[81] The "C-doped" hetero[8]circulene **176** also forms its stable radical cation upon the addition of magic blue.

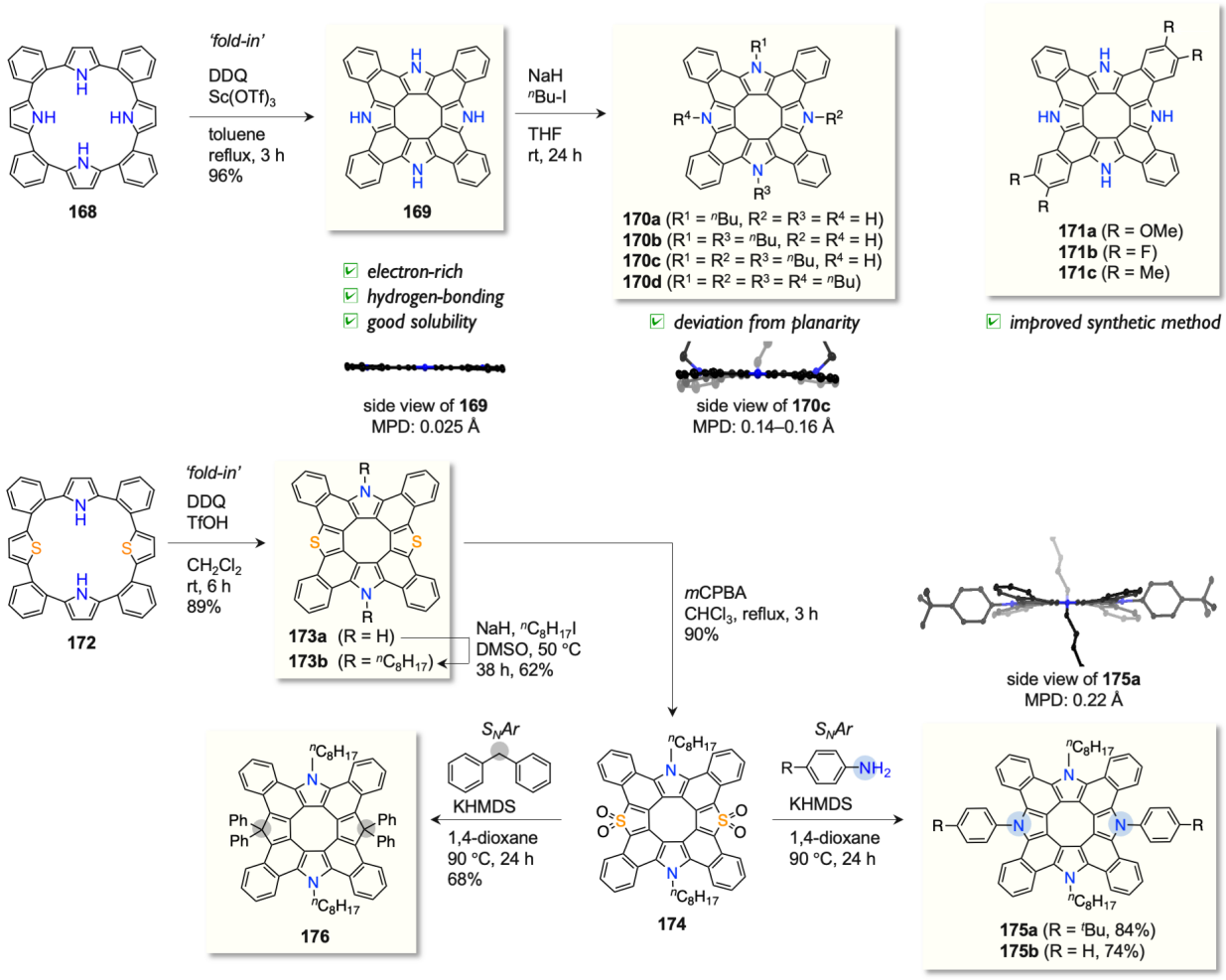

Scheme 19. Synthesis of tetraaza[8]circulene and its derivatives

In 2017, Miyake *et al*. synthesized tetraaza[8]circulenes **179a**,**b** from tetrathia[8]circulene octaoxides **178a**,**b** by nucleophilic aromatic substitution with arylamine under basic conditions (Scheme 20).[82] The planar geometries were maintained in the X-ray crystal structures though the periphery of tetraaza[8]circulenes was completely arylated and sterically congested. In **179a**,**b**, more bright emission both in solution and in solids was observed and lower oxidation potentials were revealed when compared with the sulfur analog **177a**,**b**. These observations would be derived from the absence of the heavy atom effect and the stronger electron-donating ability of nitrogen atoms compared with sulfur atoms.

The octaoxide precursors **178a**,**b** were prepared through oxidation of tetrathia[8]circulenes **177a**,**b** with *m*CPBA. Peripherally alkylated tetrathia[8]circulene octaoxides **178c–f** were also prepared by the same method.[83] In the solid state, **178c**,**d** displayed slightly saddle-distorted structures due to the longer C–S bonds compared with those of **177c**. Interestingly, **178c-f** showed aggregation-induced emission (AIE) which originated from the restriction of the dynamic motion of their saddle shaped π-frameworks in the solid state. The saddle-to-saddle inversion activation energy was estimated to be 2.4 kcal/mol.

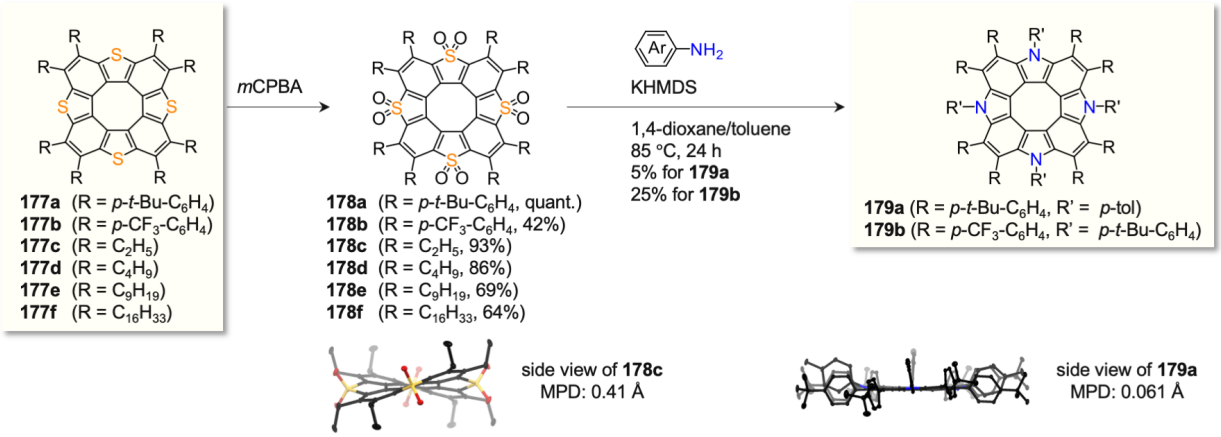

Scheme 20. Transformation of tetrathia[8]circulenes toward tetraaza[8]circulenes

In 2015, Wong *et al*. reported the synthesis of tetrathia- (**182**) and tetraselena[8]circulene (**183**) from octabromooctamethoxytetraphenylene **181** via lithiation method (Scheme 21).[84] The structure of **182** was revealed to be totally planar, while that of **183** was slightly saddle distorted due to the longer C–Se bonds (1.86 Å). They further extended this strategy to synthesize diazadithia- (**188**) and diazadiselena[8]circulene (**189**) from diaza bridged tetraphenylene **184** over four steps. X-Ray crystallographic analysis revealed that both **188** and **189** took slightly bent conformations (MPD: 0.08 Å for **188** and 0.10 Å for **189**).[85]

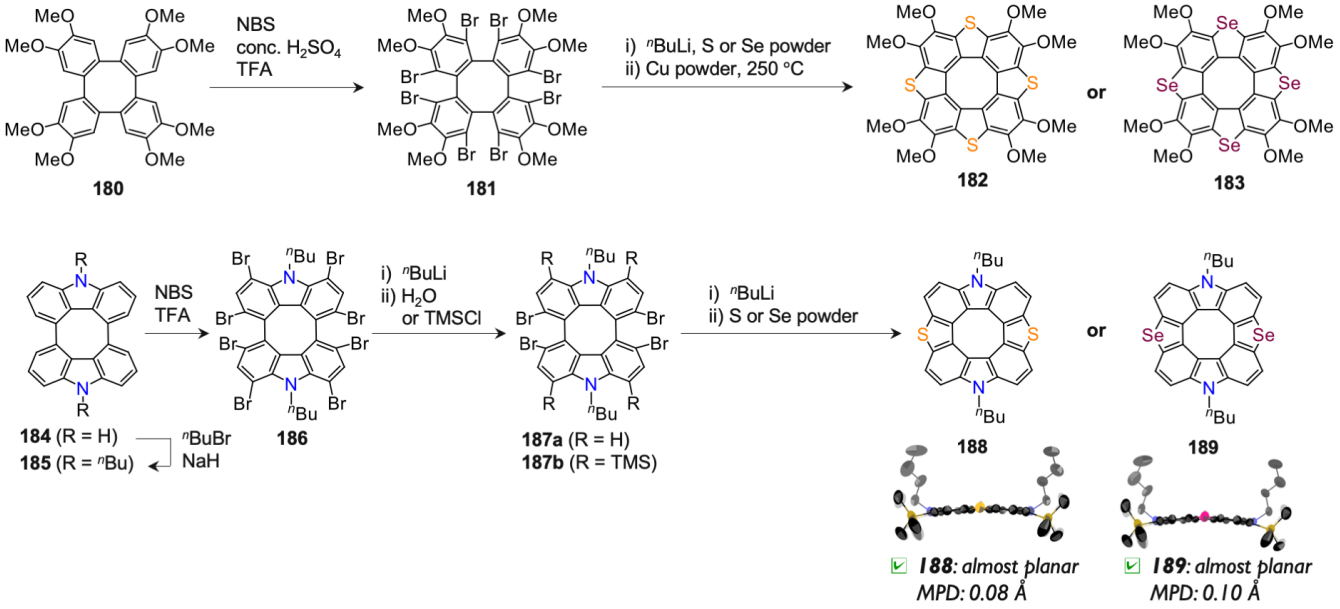

Scheme 21. Li-Mediated synthesis of hetero[8]circulenes

In 2020, Ito *et al*. synthesized π-extended diaza[8]circulene **193** by the combination of in-solution and on-surface synthesis (Scheme 22).[86] The key precursor **192** was prepared in solution via stepwise 1,3-dipolar cycloaddition reactions from dibenzocyclooctatetraene (**190**) using polycyclic azomethine ylide **18c**.[23] This is the first example of hetero[8]circulene containing six hexagons and two pentagons around the central 8-

membered ring. The planar structure of **193** on the Au(III) surface was elucidated by high-resolution CO-STM while a twisted conformation is estimated to be the most stable in the gas phase by DFT calculation. In addition, it has been revealed that the central octagon has variable bond lengths ranging from 1.42–1.69 Å. This observation indicates that the cyclooctatetraene ring is highly strained by the fully fused structure and planarization on the metal surface. In 2021, Maeda and Ema *et al.* achieved the synthesis of pristine diaza[8]circulene **199a**,**b** by a facile synthetic sequence from simple carbazole derivatives **194a-d** (Scheme 23).[87] The last step was the Buchwald-Hartwig amination reaction of *quasi*-aza[8]circulene **198** which was prepared from dimethoxy-*quasi*-aza[8]circulene **196** through demethylation and subsequent trifluoromethane sulfonylation. The structure of **199a** has been revealed to be deeply saddle distorted with its mean-plane-deviation value of 0.90 Å. They also prepared a series of extended carbazole based azahelicenes (**195a-c**, **200**, and **201a-d**) and revealed their chiroptical properties.

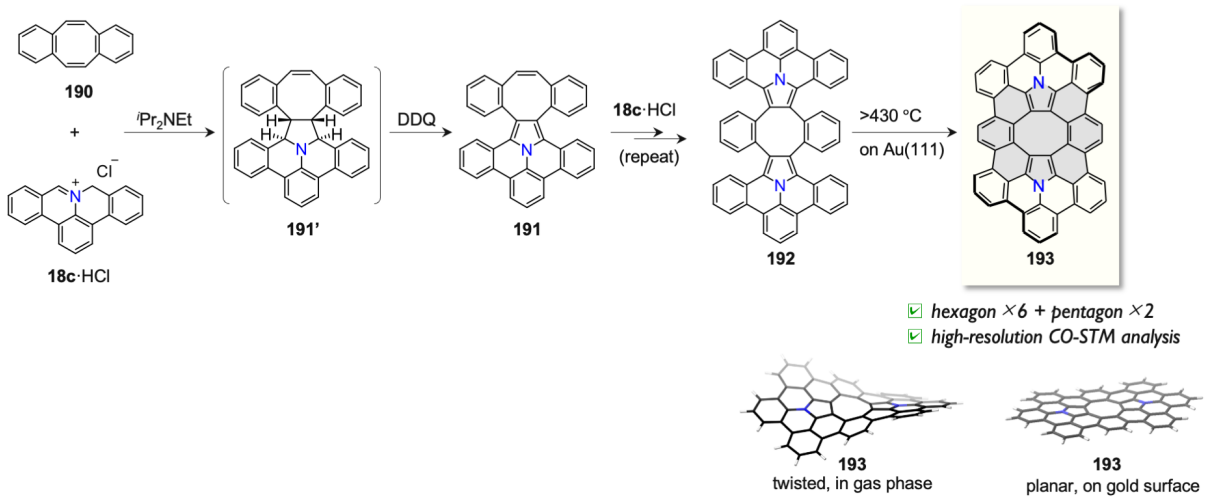

Scheme 22. Synthesis of diaza[8]circulene by the combination of in-solution and on-surface reactions

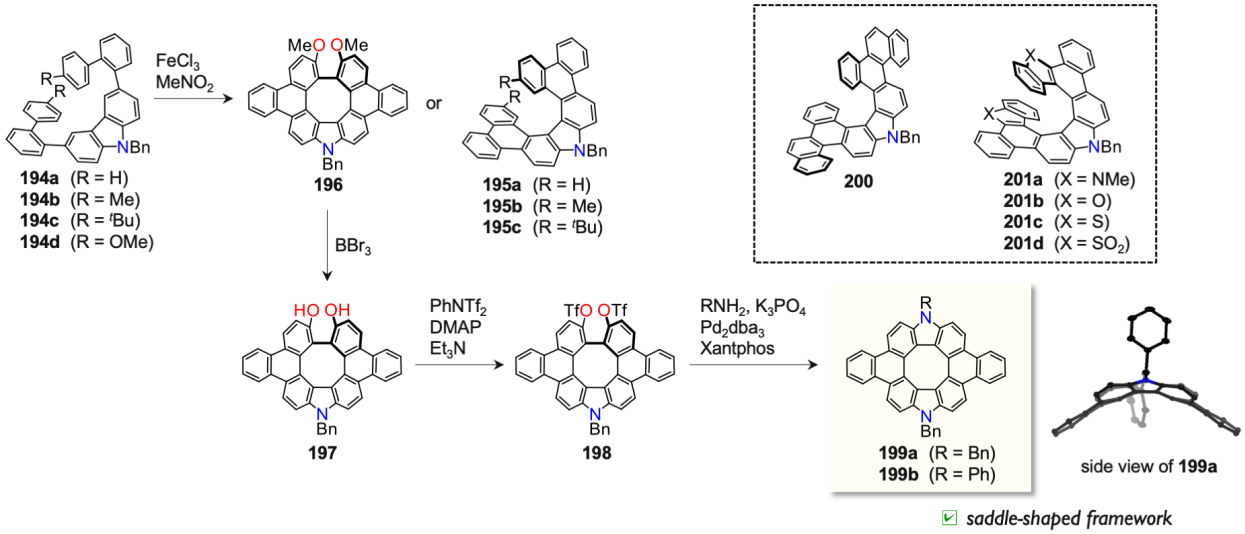

Scheme 23. Synthesis of dibenzodiaza[8]circulenes

6-2. HETERO[9]CIRCULENE

In 2021, Pittelkow *et al*. synthesized diazatrioxa[9]circulene **204** by double dehydrative oxidation of 3,6-dihydroxycarbazole derivative **152a** and glyoxal, followed by ring formation and dehydrogenation (Scheme 24).[88] This is the first example of [9]circulene. The X-ray crystal structure of **204** revealed its planar structure and significant contribution of [9]radialene-like structure. The group also attempted to prepare diazatetraoxa[10]circulene **206** by a similar reaction, but only tetrahydro[10]circulene **205** was obtained in this attempt. The structure of **205** was confirmed to be distorted V-shape. Diazatrioxa[9]circulene **204** exhibited hypsochromically-shifted lowest-energy absorption band at 410 nm as compared with diazadioxa[8]circulene **156a** (λ_{abs} = 425 nm),[74] and narrower emission band at 418 nm (Φ_F = 0.46 for **204** and 0.30 for **156a**). Tetrahydro[10]circulene **205** also exhibited similar absorption and emission, but the fluorescence quantum yield was decreased (Φ_F = 0.08) probably due to the non-radiative decay arising from the accelerated intersystem crossing rate.

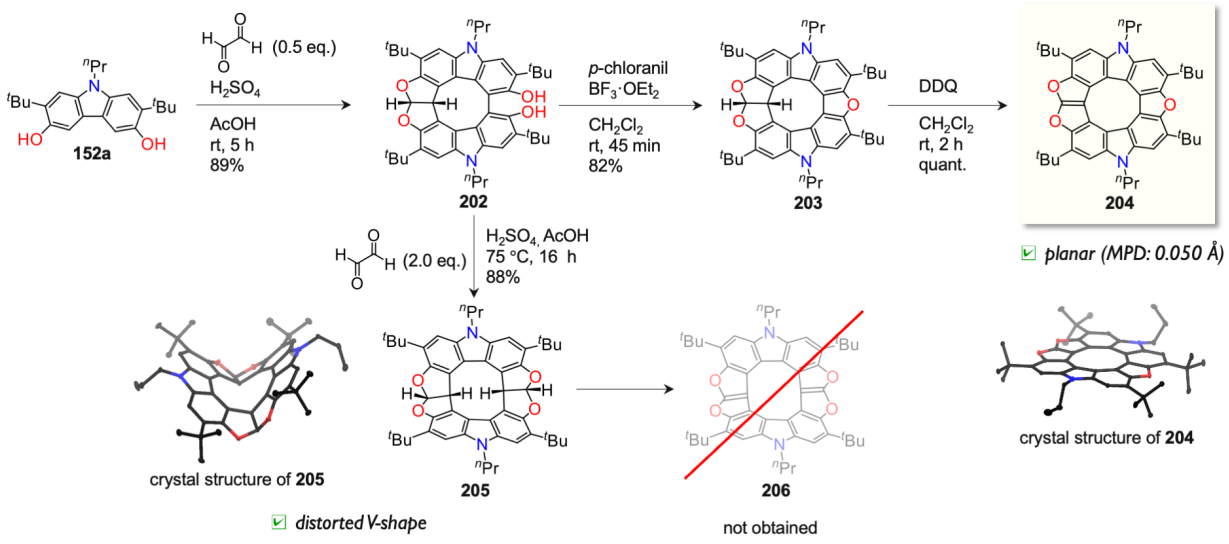

Scheme 24. Synthesis of diazatrioxa[9]circulene and attempted synthesis of [10]circulene

6-3. HETERO[10]CIRCULENE

In 2022, Tanaka *et al.* have successfully synthesized the ever largest circulene, namely, pentaaza[10]circulene (Scheme 25).[89] Pentabenzopentaaza[10]circulene **208** was obtained by fold-in type oxidative fusion of *ortho*-phenylene bridged cyclic pentapyrrole **207** with DDQ-Sc(OTf)$_3$. The fusion was not completed by the use of PIFA, which afforded closed-aza[7]helicene **209**. In addition, X-ray diffraction analysis on **208** revealed its saddle shaped conformation and [10]radialene-like electronic structure similarly to the case of tetraaza[8]circulene. According to the ^{1}H NMR and optical spectra, the structure of **208** is highly flexible even at low temperature. The saddle-to-saddle inversion dynamics were computationally investigated and a small activation barrier of 3.0 kcal/mol was elucidated.

The fold-in approach was proved to be effective in the case of *ortho*-phenylene bridged cyclic tetrapyrrole and pentapyrrole to give tetraaza[8]circulene and pentaaza[10]circulene, respectively. The further extended precursor, *i.e.,* cyclic hexapyrrole, was exposed to the same oxidative fusion reaction with DDQ-Sc(OTf)$_3$, which, however, gave closed-aza[9]helicene exclusively.[90]

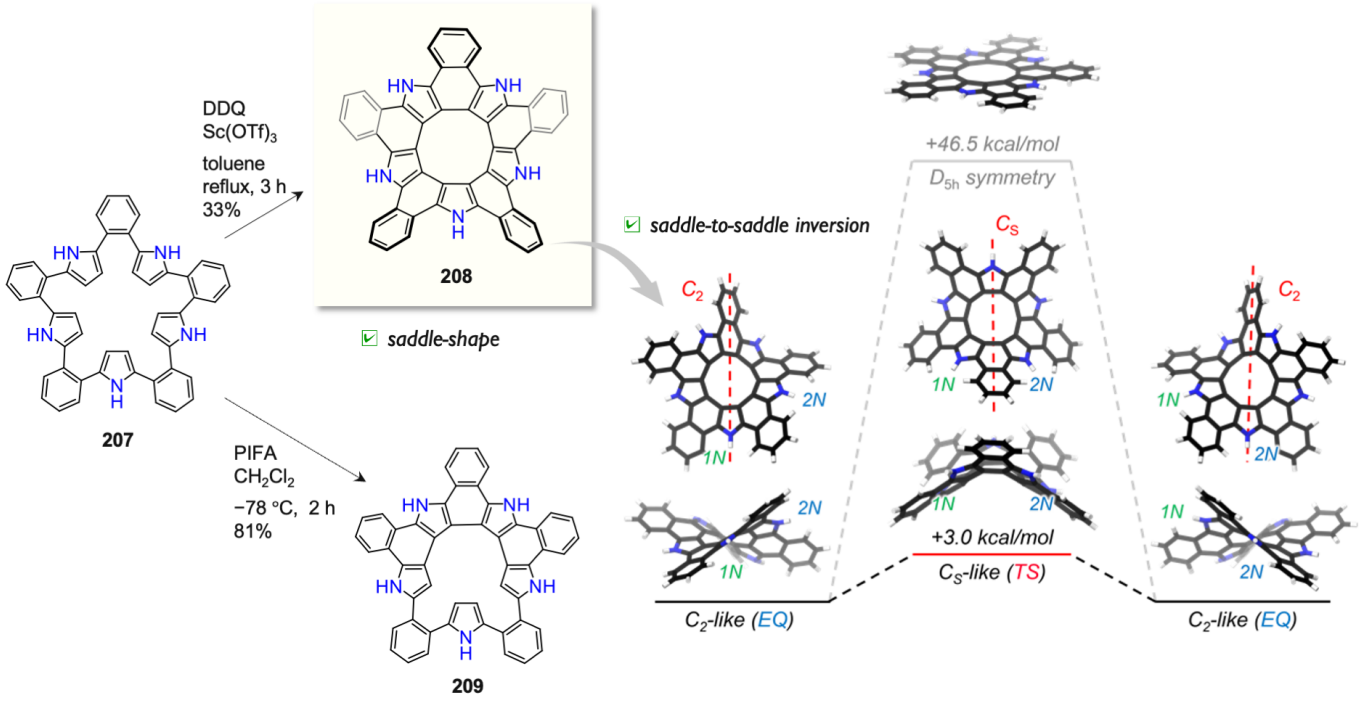

Scheme 25. Synthesis of pentaaza[10]circulene and its saddle-to-saddle inversion energy diagram

CONCLUSION

Non-planar heteronanographene is a growing area of research and several peculiar structures and properties have been reported originating from the embedded heteroatom(s) and non-planar geometry. For example, molecules endowed with the properties such as hydrogen bonding, redox responsibility, chiroptical properties, dynamic behaviors, aggregation-induced emission, and biocompatibility have been showcased in this review. Importantly, unique synthetic strategy and efficient reaction toolbox has enabled an access to state-of-the-art molecular design. Palladium catalyzed intramolecular arylative cyclization reaction has been utilized in the late stage to connect C–C bond with induction of non-planarity. Fold-in type ring closure reaction has emerged as an alternative synthetic strategy to form interior C–C bonds of polycycles, which led to the success in ever-largest hetero[10]circulene.[91] We hope that this review will motivate readers to consider challenging synthesis toward unprecedented heterafullerenes, heteracarbon nanotubes, warped heteronanographenes, and their well organized assemblies in a bottom-up manner.

ACKNOWLEDGEMENTS

This work was supported by JSPS KAKENHI Grant Numbers (20K05463 and 21H05480) for Scientific Research from MEXT. K. K. acknowledges a JSPS Fellowship for Young Scientists (No. 19J21609).

REFERENCES

1. M. A. Majewski and M. Stępień, *Angew. Chem. Int. Ed.*, 2019, **58**, 86; Chaolumen, I. A. Stepek, K. E. Yamada, H. Ito, and K. Itami, *Angew. Chem. Int. Ed.*, 2021, **60**, 23532; G. G. Miera, S. Matsubara, H. Kono, K. Murakami, and K. Itami, *Chem. Sci.*, 2022, **13**, 1848.
2. L. T. Scott, *Angew. Chem. Int. Ed.*, 2004, **43**, 4994; J. R. Sanchez-Valencia, T. Dienel, O. Gröning, I. Shorubalko, A. Mueller, N. Jansen, K. Amsharov, P. Ruffieux, and R. Fasel, *Nature*, 2014, **512**, 61; Y. Segawa, A. Yagi, K. Matsui, and K. Itami, *Angew. Chem. Int. Ed.*, 2016, **55**, 5136; J. Tomada, T. Dienel, F. Hampel, R. Fasel, and K. Amsharov, *Nat. Commun.*, 2019, **10**, 3278.
3. Y. Segawa, H. Ito, and K. Itami, *Nat. Rev. Mater.*, 2016, **1**, 15002; K. Y. Cheung, Y. Segawa, and K. Itami, *Chem. Eur. J.*, 2020, **26**, 14791; Y. Segawa, M. Kuwayama, Y. Hijikata, M. Fushimi, T. Nishihara, J. Pirillo, J. Shirasaki, N, Kubota, and K. Itami, *Science*, 2019, **365**, 272; S. Nishigaki, Y. Shibata, A. Nakajima, H. Okajima, Y. Masumoto, T. Osawa, A. Muranaka, H. Sugiyama, A. Horikawa, H. Uekusa, H. Koshino, M. Uchiyama, A. Sakamoto, and K. Tanaka, *J. Am. Chem. Soc.*, 2019, **141**, 14955.
4. I. R. Márquez, S. Castro-Fernández, A. Millán, and A. G. Campaña, *Chem. Commun.*, 2018, **54**, 6705; M. Rickhaus, M. Mayor, and M. Juríĉek, *Chem. Soc. Rev.*, 2017, **46**, 1643; C. Li, Y. Yang, and Q. Miao, *Chem. Asian J.*, 2018, **13**, 884; A. Tsurusaki and K. Kamikawa, *Chem. Lett.*, 2021, **50**, 1913.
5. R. Kumar, H. Aggarwal, and A. Srivastava, *Chem. Eur. J.*, 2020, **26**, 10653.
6. Y.-T. Wu and J. S. Siegel, *Chem. Rev.*, 2006, **106**, 4843; V. M. Tsefrikas and L. T. Scott, *Chem. Rev.*, 2006, 106, 4868; S. Higashibayashi and H. Sakurai, *Chem. Lett.*, 2011, **40**, 122; T. Amaya and T. Hirao, *Chem. Commun.*, 2011, **47**, 10524; B. M. Schmidt and D. Lentz, *Chem. Lett.*, 2014, **43**, 171.
7. W. E. Barth and R. G. Lawton, *J. Am. Chem. Soc.*, 1966, **88**, 380; R. G. Lawton and W. E. Barth, *J. Am. Chem. Soc.*, 1971, **93**, 1730.
8. H. Sakurai, T. Daiko, and T. Hirao, *Science*, 2003, **301**, 1878.
9. M. Stępień, E. Gońka, M. Żyła, and N. Sprutta, *Chem. Rev.*, 2017, **117**, 3479; A. Borissov, Y. K. Maurya, L. Moshniaha, W.-S. Wong, M. Żyła-Karwowska, and M. Stępień, *Chem. Rev.*, 2022, **122**, 565.
10. M. Stępień, *Synlett*, 2013, 1316; X.-Y. Wang, J.-Y. Wang, and J. Pei, *Chem. Eur. J.*, 2015, **21**, 3528; A. Narita, X.-Y. Wang, X. Feng, and K. Müllen, *Chem. Soc. Rev.*, 2015, **44**, 6616; M. Saito, H. Shinokubo, and H. Sakurai, *Mat. Chem. Front.*, 2018, **2**, 635; M. Hirai, N. Tanaka, M. Sakai, and S.

Yamaguchi, *Chem. Rev.*, 2019, **119**, 8291; S. Hiroto, *Chem*. *Lett*., 2020, **50**, 1146; M. Grzybowski, B. Sadowski, H. Butenchön, and D. T. Gryko, *Angew. Chem. Int. Ed.*, 2020, **59**, 2998; W. Wang and X. Shao, *Org. Biomol. Chem.*, 2021, **19**, 101.

11. R. C. Haddon, *J*. *Am*. *Chem*. *Soc*., 1978, **109**, 1676.
12. T. J. Seiders, K. K. Baldridge, G. H. Grube, and J. S. Siegel, *J*. *Am*. *Chem*. *Soc*., 2001, **123**, 517; E. Solel, D. Pappo, O. Reany, T. Mejuch, R. Gershoni-Poranne, M. Botoshansky, A. Stanger, and E. Keinan, *Chem. Sci.*, 2020, **11**, 13015.
13. L. T. Scott, M. M. Hashemi, D. T. Meyer, and H. B. Warren, *J*. *Am*. *Chem*. *Soc*., 1991, **113**, 7082; L. T. Scott, P.-C. Cheng, M. M. Hashemi, M. S. Bratcher, and H. B. Warren, *J*. *Am*. *Chem*. *Soc*., 1997, **119**, 10963; L. T. Scott, M. M. Hashemi, and M. S. Bratcher, *J*. *Am*. *Chem*. *Soc*., 1992, **114**, 1920.
14. R. F. C. Brown, Pyrolytic Methods in Organic Chemistry: Application of Flow and Flash Vacuum Pyrolytic Techniques; Academic Press: New York, 1980; L. T. Scott, *Pure Appl. Chem.*, 1996, **68**, 291.
15. A. M. Butterfield, B. Gilomen, and J. S. Siegel, *Org*. *Process Res*. *Dev*., 2012, **16**, 664.
16. T. Yong, G. Báti, F. García, and M. C. Stuparu, *Nat*. *Commun*., 2021, **12**, 5187.
17. J. C. Hummelen, B. Knight, J. Paviovich, R. Gonzalez, and F. Wudi, *Science*, 1995, **269**, 1554; B. Number and A. Hirsch, *Chem*. *Commun*., 1996, 1421; M. Keshavarz-K., R. Gonzalez, R. G. Hicks, G. Srdanov, V. I. Srdanov, T. G. Collins, J. C. Hummelen, C. Bellavia-Lund, J. Pavlovich, F. Wudl, and K. Holcze, *Nature*, 1996, **383**, 147; G. Zhang, S. Huang, Z. Xiao, Q. Chen, L. Gan, and Z. Wang, *J*. *Am*. *Chem*. *Soc*., 2008, **130**, 12614.
18. H. A. Reisch, M. S. Bratcher, and L. T. Scott, *Org*. *Lett*., 2000, **2**, 1427; V. M. Tsefrikas, S. Arns, P. M. Merner, C. C. Warford, B. L. Merner, L. T. Scott, and G. J. Bodwell, *Org*. *Lett*., 2006, **8**, 5195.
19. V. M. Tsefrikas, A. K. Greene, and L. T. Scott, *Org*. *Chem*. *Front*., 2017, **4**, 688.
20. S. Nakatsuka, N. Yasuda, and T. Hatakeyama, *J*. *Am*. *Chem*. *Soc*., 2018, **140**, 13562.
21. H. Yokoi, Y. Hiraoka, S. Hiroto, D. Sakamaki, S. Seki, and H. Shinokubo, *Nat*. *Commun*., 2015, **6**, 8215.
22. S. Ito, Y. Tokimaru, and K. Nozaki, *Angew*. *Chem*. *Int*. *Ed*., 2015, **54**, 7256.
23. S. Ito, Y. Tokimaru, and K. Nozaki, *Chem. Commun.*, 2015, **51**, 221.
24. R. Berger, M. Wagner, X. Feng, and K. Müllen, *Chem. Sci.*, 2015, **6**, 436.
25. H. Yokoi, S. Hiroto, and H. Shinokubo, *J*. *Am*. *Chem*. *Soc*., 2018, **140**, 4649.
26. H. Yokoi, S. Hiroto, D. Sakamaki, S. Seki, and H. Shinokubo, *Chem*. *Sci*., 2018, **9**, 819; M. Takeda, S. Hiroto, H. Yokoi, S. Lee, D. Kim, and H. Shinokubo, *J*. *Am*. *Chem*. *Soc*., 2018, **140**, 6336.
27. Q.-Q. Li, Y. Hamamoto, G. Kwek, B. Xing, Y. Li, and S. Ito, *Angew*. *Chem*. *Int*. *Ed*., 2022, **61**, e202112638.

28. X. Li, F. Kang, and M. Inagaki, *Small*, 2016, **12**, 3206; E. Nestoros and M. C. Stuparu, *Chem. Commun.*, 2018, **54**, 6503; E. M. Muzammil, D. Halilovic, and M. C. Stuparu, *Commun. Chem.*, 2019, **2**, 58; J. Kang, D. Miyajima, T. Mori, Y. Inoue, Y. Itoh, and T. Aida, *Science*, 2015, **347**, 646; S. H. Mahadevegowda and M. C. Stuparu, *ACS Omega*, 2017, **2**, 4964; T. Nagano, K. Nakamura, Y. Tokimaru, S. Ito, D. Miyajima, T. Aida, and K. Nozaki, *Chem*. *Eur*. *J*., 2018, **24**, 14075.
29. Y. Tokimaru, S. Ito, and K. Nozaki, *Angew*. *Chem*. *Int*. *Ed*., 2017, **56**, 15560.
30. Y. Tokimaru, S. Ito, and K. Nozaki, *Angew*. *Chem*. *Int*. *Ed*., 2018, **57**, 9818.
31. Y. Wang, O. Allemann, T. S. Balaban, N. Vanthuyne, A. Linden, K. K. Baldridge, and J. S. Siegel, *Angew*. *Chem*. *Int*. *Ed*., 2018, **57**, 6470.
32. X. Tian, L. M. Roch, N. Vanthuyne, J. Xu, K. K. Baldridge, and J. S. Siegel, *Org. Lett.*, 2019, **21**, 3510.
33. X. Tian, S. Chaiworn, J. Xu, N. Vanthuyne, K. K. Baldridge, and J. S. Siegel, *Org. Chem. Front.*, 2021, **8**, 3653.
34. M. Saha, Y.-H. Bao, and C. Zhou, *Chem*. *Lett*., 2018, **47**, 1383.
35. K. Kise, S. Ooi, A. Osuka, and T. Tanaka, *Asian J. Org. Chem.*, 2021, **10**, 537.
36. K. Kise, S. Ooi, H. Saito, H. Yorimitsu, A. Osuka, and T. Tanaka, *Angew. Chem. Int. Ed.*, 2022, **61**, e202112589.
37. L. Meng, T. Fujikawa, M. Kuwayama, Y. Segawa, and K. Itami, *J. Am. Chem. Soc.*, 2016, **138**, 10351.
38. H. Sakurai, T. Daiko, H. Sakane, T. Amaya, and T. Hirao, *J. Am. Chem. Soc.*, 2005, **127**, 11580; R. Tsuruoka, S. Higashibayashi, T. Ishikawa, S. Toyota, and H. Sakurai, *Chem. Lett.*, 2010, **39**, 646; T. Amaya, M. Hifumi, M. Okada, Y. Shimizu, T. Moriuchi, K. Segawa, Y. Ando, and T. Hirao, *J. Org. Chem.*, 2011, **76**, 8049.
39. X. Li and X. Shao, *Synlett*, 2014, **25**, 1795; M. Saito, S. Furukawa, J. Kobayashi, and T. Kawashima, *Chem*. *Rec*., 2016, **16**, 64.
40. Q. Tan, S. Higashibayashi, S. Karangi, and H. Sakurai, *Nat*. *Commun*., 2012, **3**, 891.
41. P. Kaewmati, Q. Tan, S. Higashibayashi, Y. Yakiyama, and H. Sakurai, *Chem*. *Lett*., 2017, **46**, 146.
42. Q. Tan, P. Kaewmati, S. Higashibayashi, M. Kawano, Y. Yakiyama, and H. Sakurai, *Bull*. *Chem*. *Soc*. *Jpn*., 2018, **91**, 531.
43. K. Imamura, K. Takimiya, T. Otsubo, and Y. Aso, *Chem*. *Commun*., 1999, 1859.
44. X. Li, Y. Zhu, J. Shao, B. Wang, S. Zhang, Y. Shao, X. Jin, X. Yao, R. Fang, and X. Shao, *Angew*. *Chem*. *Int*. *Ed*., 2014, **53**, 535.
45. S. Wang, X. Li, X. Hou, Y. Sun, and X. Shao, *Chem*. *Commun*., 2016, **52**, 14486.
46. X. Li, Y. Zhu, J. Shao, L. Chen, S. Zhao, B. Wang, S. Zhang, Y. Shao, H.-L. Zhang, and X. Shao, *Angew*. *Chem*. *Int*. *Ed*., 2015, **54**, 267; Q. Tan, D. Zhou, T. Zhang, B. Liu, and B. Xu, *Chem. Commun.*,

2017, **53**, 10279; S. Wang, J. Shang, C. Yan, W. Wang, C. Yuan, H.-L. Zhang, and X. Shao, *Org. Chem. Front.*, 2019, **6**, 263; S. Wang, C. Yan, J. Shang, W. Wang, C. Yuan, H.-L. Zhang, and X. Shao, *Angew. Chem. Int. Ed.*, 2019, **58**, 3819; M. Jiang, J. Guo, B. Liu, Q. Tan, and B. Xu, *Org. Lett.*, 2019, **21**, 8328.

47. S. Furukawa, J. Kobayashi, and T. Kawashima, *J. Am. Chem. Soc*., 2009, **131**, 14192.
48. S. Furukawa, Y. Suda, J. Kobayashi, T. Kawashima, T. Tada, S. Fujii, M. Kiguchi, and M. Saito, *J. Am. Chem. Soc*., 2017, **139**, 5787.
49. F. Chen. T. Tanaka, and A. Osuka, *Chem. Commun*., 2017, **53**, 2705.
50. J. Shang, R. Wang, C. Yuan, Z. Liu, H.-L. Zhang, and X. Shao, *Angew. Chem. Int. Ed*., 2022, **61**, e202117504.
51. T. Tanikawa, M. Saito, J. D. Guo, S. Nagase, and M. Minoura, *Eur. J. Org. Chem*., 2012, 7135.
52. D. Zhou, Y. Gao, B. Liu, Q. Tan, and B. Xu, *Org. Lett.*, 2017, **19**, 4628.
53. M. Saito, T. Tanikawa, T. Tajima, J. D. Guo, and S. Nagase, *Tetrahedron*, 2010, **51**, 672.
54. D. Myśliwiec and M. Stępień, *Angew. Chem. Int. Ed*., 2013, **52**, 1713.
55. M. Zhao, S. H. Pun, Q. Gong, and Q. Miao, *Angew. Chem. Int. Ed*., 2021, **60**, 24124.
56. S. Higashibayashi, P. Pandit, R. Haruki, S.-i. Adachi, and R. Kumai, *Angew. Chem. Int. Ed*., 2016, **55**, 10830.
57. Y. Morimoto, Y. H. Koo, K. Otsubo, H. Kitakado, S. Seki, A. Osuka, and T. Tanaka, *Angew. Chem. Int. Ed*., 2022, **61**, e202200341.
58. S. Mishra, M. Krzeszewski, C. A. Pignedoli, P. Ruffieux, R. Fasel, and D. T. Gryko, *Nat. Commun*., 2018, **9**, 1714.
59. M. Krzeszewski, Ł. Dobrzycki, A. L. Sobolewski, M. K. Cyrański, and D. T. Gryko, *Angew. Chem. Int. Ed*., 2021, **60**, 14998.
60. M. Lazerges, M. Jouini, P. Hapiot, P. Guiriec, and P.-C. Lacaze, *J. Phys. Chem. A*, 2003, **107**, 5042.
61. M. Takase, V. Enkelmann, D. Sebastiani, M. Baumgarten, and K. Müllen, *Angew. Chem. Int. Ed*., 2007, **46**, 5524.
62. K. Oki, M. Takase, N. Kobayashi, and H. Uno, *J. Org. Chem*., 2021, **86**, 5102.
63. E. Gońka, P. J. Chmielewski, T. Lis, and M. Stępień, *J. Am. Chem. Soc*., 2014, **136**, 16399.
64. K. Oki, M. Takase, S. Mori, and H. Uno, *J. Am. Chem. Soc*., 2019, **141**, 16255.
65. M. Żyła-Karwowska, H. Zhylitskaya, J. Cybińska, T. Lis, P. J. Chmielewski, and M. Stępień, *Angew. Chem. Int. Ed*., 2016, **55**, 14658.
66. Y. Sasaki, M. Takase, N. Kobayashi, S. Mori, K. Ohara, T. Okujima, and H. Uno, *J. Org. Chem*., 2021, **86**, 4290.
67. K. Oki, M. Takase, S. Mori, A. Shiotari, Y. Sugimoto, K. Ohara, T. Okujima, and H. Uno, *J. Am.*

Chem. *Soc*., 2018, **140**, 10430.

68. R. Scholl and K. Meyer, *Ber. Dtsch. Chem. Ges. A*, 1932, **65**, 902.
69. Bharat, R. Bhola, T. Bally, A. Valente, M. K. Cyrański, Ł. Dobrzycki, S. M. Spain, P. Rempała, M. R. Chin, and B. T. King, *Angew. Chem. Int. Ed.*, 2010, **49**, 399.
70. K. Yamamoto, H. Sonobe, H. Matsubara, M. Saito, S. Okamoto, and K. Kitaura, *Angew. Chem., Int. Ed. Engl.*, 1996, **35**, 69.
71. C.-N. Feng, M.-Y. Kuo, and Y.-T. Wu, *Angew. Chem. Int. Ed.*, 2013, **52**, 7791.
72. Y. Miyake and H. Shinokubo, *Chem*. *Commun*., 2020, **56**, 15605; T. Hensel, N. N. Andersen, M. Plesner, and M. Pittelkow, *Synlett*, 2016, **27**, 498; G. V. Baryshnikov, B. F. Minaev, and V. A. Minaeva, *Russ. Chem. Rev.*, 2015, **84**, 455.
73. C. B. Nielsen, T. Brock-Nannestad, P. Hammershøj, T. K. Reenberg, M. Schau-Magnussen, D. Trpcevski, T. Hensel, R. Salcedo, G. V. Baryshnikov, B. F. Minaev, and M. Pittelkow, *Chem*. *Eur*. *J*., 2013, **19**, 3898.
74. T. Hensel, D. Trpcevski, C. Lind, R. Grosjean, P. Hammershøj, C. B. Nielsen, T. Brock-Nannestad, B. E. Nielsen, M. Schau-Magnussen, B. Minaev, G. V. Baryshnikov, and M. Pittelkow, *Chem*. *Eur*. *J*., 2013, **19**, 17097.
75. B. Lousen, S. K. Pedersen, P. Bols, K. H. Hansen, M. R. Pedersen, O. Hammerich, S. Bondarchuk, B. Minaev, G. V. Baryshnikov, H. Ågren, and M. Pittelkow, *Chem. Eur. J.*, 2020, **26**, 4935.
76. F. Chen, T. Tanaka, T. Mori, and A. Osuka, *Chem*. *Eur*. *J*., 2018, **24**, 7489; Y. Matsuo, F. Chen. K. Kise, T. Tanaka, and A. Osuka, *Chem*. *Sci*., 2019, **10**, 11006.
77. F. Chen, Y. S. Hong, S. Shimizu, D. Kim, T. Tanaka, and A. Osuka, *Angew*. *Chem*. *Int*. *Ed*., 2015, **54**, 10639.
78. F. Chen, Y. S. Hong, D. Kim, T. Tanaka, and A. Osuka, *ChemPlusChem*, 2017, **82**, 1048.
79. Y. Morimoto, F. Chen, Y. Matsuo, K. Kise, T. Tanaka, and A. Osuka, *Chem*. *Asian J*., 2021, **16**, 648.
80. Y. Matsuo, T. Tanaka, and A. Osuka, *Chem*. *Eur*. *J*., 2020, **26**, 8144.
81. Y. Matsuo, T. Tanaka, and A. Osuka, *Chem*. *Lett*., 2019, **49**, 959.
82. Y. Nagata, S. Kato, Y. Miyake, and H. Shinokubo, *Org*. *Lett*., 2017, **19**, 2718.
83. H. Murase, Y. Nagata, S. Akahori, H. Shinokubo, and Y. Miyake, *Chem. Asian J.*, 2020, **15**, 3873.
84. X. Xiong, C.-L. Deng, B. F. Minaev, G. V. Baryshnikov, X.-S. Peng, and H. N. C. Wong, *Chem. Asian J.*, 2015, **10**, 969.
85. X. Xiong, C.-L. Deng, Z. Li, X.-S. Peng, and H. N. C. Wong, *Org*. *Chem*. *Front*., 2017, **4**, 682.
86. K. Nakamura, Q.-Q. Li, O. Krejčí, A. S. Foster, K. Sun, S. Kawai, and S. Ito, *J*. *Am*. *Chem*. *Soc*., 2020, **142**, 11363.
87. C. Maeda, S. Nomoto, K. Akiyama, T. Tanaka, and T. Ema, *Chem. Eur. J.*, 2021, **27**, 15699.

88. S. K. Pedersen, K. Eriksen, H. Ågren, B. F. Minaev, N. N. Karaush-Karmazin, O. Hammerich, G. V. Baryshnikov, and M. Pittelkow, *J. Am. Chem. Soc.*, 2020, **142**, 14058.
89. Y. Matsuo, K. Kise, Y. Morimoto, A. Osuka, and T. Tanaka, *Angew. Chem. Int. Ed.*, 2022, **61**, e202116789.
90. F. Chen, T. Tanaka, Y. S. Hong, T. Mori, D. Kim, and A. Osuka, *Angew. Chem. Int. Ed.*, 2017, **56**, 14688.
91. T. Tanaka, *Bull. Chem. Soc. Jpn.*, 2022, **95**, 602.

Prof. Dr. Takayuki Tanaka completed his Ph.D. at the Department of Chemistry, Graduate School of Science, Kyoto University (Japan) in 2012. He worked as a Postdoctoral Fellow for Research Abroad of the Japan Society for the Promotion of Science at Boston College before moving back to the group of Professor Atsuhiro Osuka in Kyoto University as an assistant professor in 2013. In 2021, he was promoted to an associate professor in the Department of Molecular Engineering, Graduate School of Engineering, Kyoto University. He received the 70th Chemical Society of Japan Award for Young Chemists, Thieme Chemistry Journals Award 2021, and the 31st Inoue Science Research Award for Young Scientists. His research interest is in the area of synthetic organic chemistry and physical organic chemistry of novel porphyrinoids and heteroatom embedded nanographene molecules.

Dr. Koki Kise completed his Ph.D. at the Department of Chemistry, Graduate School of Science, Kyoto University (Japan) in 2022 under the supervision of Prof. Dr. Atsuhiro Osuka, Prof. Dr. Shohei Saito, and Prof. Dr. Takayuki Tanaka. He found a job with a chemical company in 2022. His research interest is in the area of synthetic organic chemistry and physical organic chemistry of novel heteroatom doped bowl shaped molecules.